chain gene promoter, and intronic enhancer elements (Fig. 3A). Increased G5PR expression was confirmed in G5PR^{Tg} murine splenocytes by RT-PCR and Western blot analysis. No obvious difference was observed in the number or proportion of lymphoid cells or in the development of B cells in the bone marrow and the spleen at 8–12 wk after birth, in comparison with that in WT littermates (Supplemental Fig. 2). Although an apparent inhibition of JNK activation was noted after αIgM stimulation (Fig. 3B),

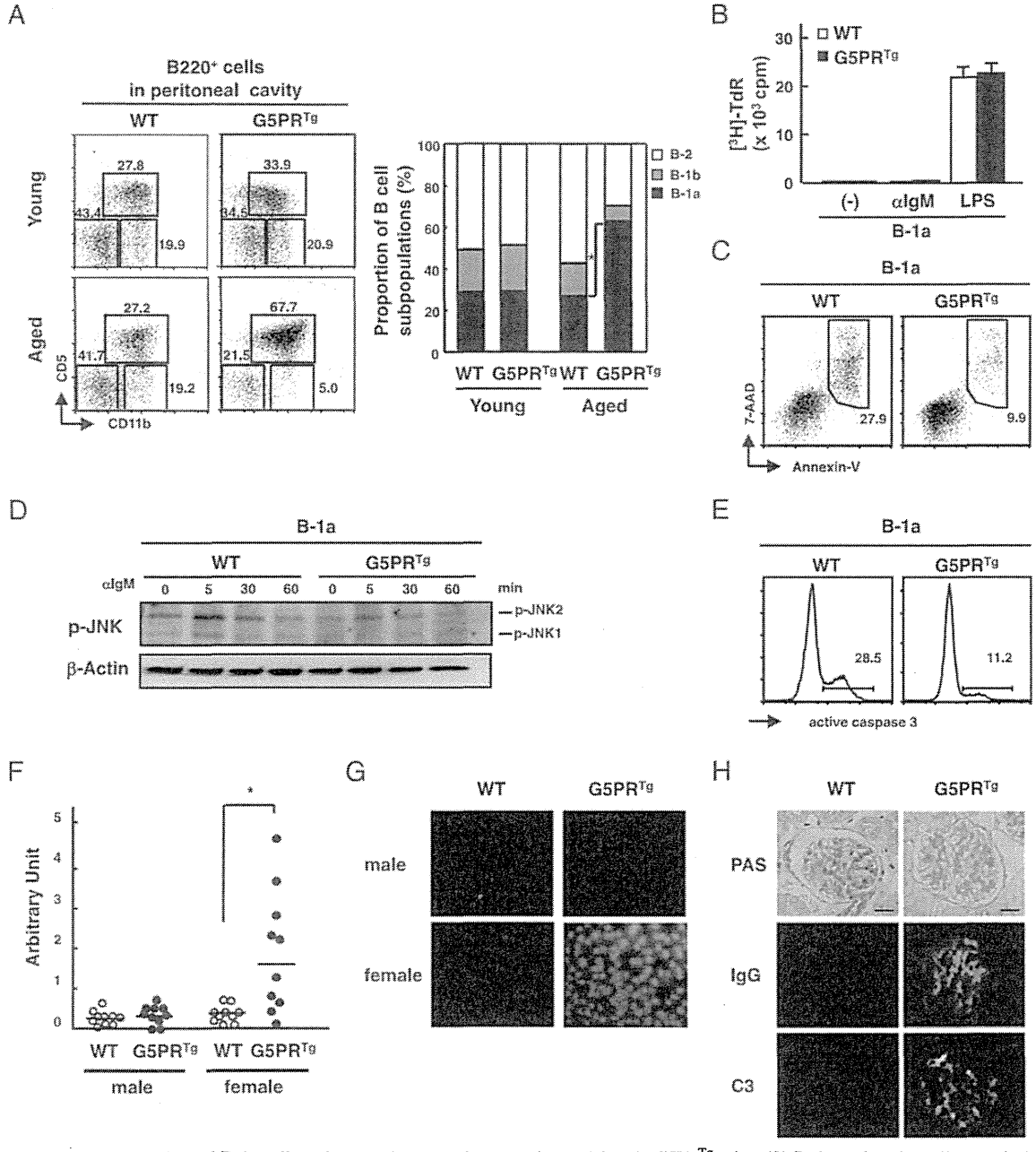

FIGURE 5. Increase in peritoneal B-1a cells and an autoimmune phenotype in aged female G5PR^{Tg} mice. (**A**) Peritoneal cavity cells were isolated from young (8–12 wk) and aged (>40 wk) G5PR^{Tg} mice or littermates and stained with anti–CD5-PE, anti–CD11b-FITC, and anti-B220 allophycocyanin-conjugated Abs. The proportion of B-1a (CD5$^+$CD11b$^+$B220$^+$), B-1b (CD5$^-$CD11b$^+$B220$^+$), and B-2 (CD5$^-$CD11b$^-$B220$^+$) cells was analyzed by flow cytometry. Results are representative of three independent experiments (*left panel*). The proportion of B-1a, B-1b, and B-2 cells is shown as the mean of each group (*right panel*, $n = 5$). (**B**) Proliferation of peritoneal B-1a cells. Peritoneal B-1a (CD5$^+$B220$^+$) cells of G5PR^{Tg} mice or littermates ($n = 3$ per each) were isolated using a JSAN Cell Sorter and stimulated with αIgM and LPS for 48 h. Incorporation of [^{3}H]-TdR was measured as in Fig. 3E. (**C**) Peritoneal B-1a (CD5$^+$B220$^+$) cells of G5PR^{Tg} mice or littermates ($n = 6$) were isolated using a JSAN Cell Sorter and stimulated with αIgM for 24 h. Apoptotic cells were identified with Annexin V^{FITC} and 7-AAD staining. Results are representative of four independent experiments. (**D**) Peritoneal B-1a cells from G5PR^{Tg} mice or littermates were stimulated with αIgM for the indicated times, and JNK phosphorylation was monitored by immunoblotting for p-JNK. Results are representative of two independent experiments. (**E**) Peritoneal B-1a cells from G5PR^{Tg} mice or littermates were stimulated with αIgM for 24 h. Active caspase 3 was stained with mAb and detected by flow cytometry. Results are representative of two independent experiments. (**F**) Anti-dsDNA Ab titers of sera from young and aged G5PR^{tg} mice or WT littermates ($n = 10$, respectively) were measured by ELISA. Results are shown as the mean ± SD. *$p < 0.05$. (**G**) Anti-nuclear Abs in the aged mouse sera were detected by staining of HEp-2 cells. Alexa 488-conjugated anti-IgG Ab was used for the detection of anti-nuclear Ab. Results are representative of three independent experiments. Original magnification ×200. (**H**) Detection of immune complex deposition in the kidney. Kidney sections from female G5PR^{Tg} mice and littermates were stained with periodic acid-Schiff (PAS), anti-IgG Ab or anti-C3 Ab, respectively. Scale bars, 100 μm.

splenic B cells from G5PR^{Tg} mice showed neither an alteration in active caspase 3 (Fig. 3C) nor a difference in BCR-mediated AICD, in comparison with WT B cells (Fig. 3D). The proliferation potential of splenic B cells from G5PR^{Tg} mice was similar to that of WT mice following stimulation with αIgM or LPS in vitro (Fig. 3E). These results imply that increased G5PR expression does not cause a marked change in the development of mature peripheral B cells or the survival of B cells under nonimmunized conditions.

However, when we immunized G5PR^{Tg} mice with TD-Ag SRBC, we observed an altered formation of PNA$^+$ splenic GCs surrounded by IgD$^+$ B cells. The number of GCs was similar but significantly larger in comparison with that in WT mice (Fig. 4A). Following immunization with NP-CGG in alum, the frequency of mature GC B cells expressing B220$^+$Fas$^+$GL7$^+$ markers was significantly increased, as compared with that in WT mice (Fig. 4B). However, the increase of mature GC B cells did not result in an increase in NIP-specific B cells. Instead, we observed a decrease in strongly Ag-binding B cells in G5PR^{Tg} mice (Fig. 4C). The decrease of high-affinity Ag-binding B cells was also confirmed in the sera by a convenient affinity measurement, using the differential ELISA. The levels of high-affinity Abs measured by NP_2-BSA were unchanged in G5PR^{Tg} mice compared with WT mice, but the low-affinity Ab titers measured by NP_{25}-BSA were significantly higher in G5PR^{Tg} mice than in WT mice (Fig. 4D). The overall affinity of the sera was calculated by the ratio of each measurement, NP_2/NP_{25}. These results suggest that increased G5PR expression in G5PR^{Tg} mice affects the selection of Ag-binding B cells in GCs, perhaps by altering the threshold of BCR-mediated signal during the generation of high-affinity Ag-specific B cells.

T_{FH} cells may play an important role in B cell maturation in GCs, in association with G5PR expression. The *g5pr* transcripts were upregulated in T_{FH} cells in G5PR^{Tg} mice. However, Ag immunization induced a similar number of T_{FH} (CD4$^+$PD-1$^+$ CXCR5$^+$) cells in the spleens of G5PR^{Tg} mice comparable to that in WT mice (Supplemental Fig. 3). Although we have not neglected the effects of G5PR on T_{FH} cells in G5PR^{Tg} mice, the G5PR overexpression on B cells is most likely the cause of impaired affinity–maturation of Ag-specific GC B cells in vivo.

Effect of increased G5PR expression upon the number of peritoneal B-1a cells after aging

A more dramatic change was observed in the G5PR^{Tg} mice after aging. Aged mice (>40 wk), in comparison with WT littermates, showed a marked increase in B-1a cells in the peritoneal cavity (Fig. 5A). The proportion of B-1a (CD5$^+$CD11b$^+$B220$^+$) cells, but not B-1b (CD5$^-$CD11b$^+$B220$^+$) and B-2 (CD5$^-$CD11b$^-$B220$^+$) cells, in the peritoneal cavity increased significantly in aged female G5PR^{Tg} mice, although no increase was observed in mice at a young time point. To examine the proliferation capacity of B-1 cells, we isolated sufficient numbers of peritoneal B-1a cells from aged mice only and used them for comparison in the proliferation assay (Fig. 5B). B-1a cells from both G5PR^{Tg} and WT mice did not respond to αIgM stimulation but did respond well to LPS stimulation. As LPS is an efficient stimulator of B-1 cells, compared with αIgM Ab in vitro (28), we concluded that the proliferation capacity of B-1a cells is not impaired in G5PR^{Tg} mice (Fig. 5B). However, peritoneal B-1a cells, but not splenic B-2 cells, from aged female G5PR^{Tg} mice were resistant to BCR-mediated AICD in vitro, in comparison with those of WT mice (Fig. 5*C*, Supplemental Fig. 4). JNK activation by αIgM stimulation was lower in peritoneal B-1a cells from WT mice, but was further decreased in the G5PR^{Tg} mice during the period from 5 to 60 min after stimulation (Fig. 5D). The peritoneal B-1a cells from aged female G5PR^{Tg} mice, in comparison with those from WT mice, also showed suppression in activation of caspase 3 after αIgM stimulation in vitro (Fig. 5E), suggesting that the peritoneal B-1a cells from G5PR^{Tg} mice are under the continued suppression of BCR-mediated JNK activation, most likely leading to AICD.

As a persistent increase of B-1a cells might be associated with the development of autoimmunity, we examined autoantibody production in the aged G5PR^{Tg} mice by ELISA with dsDNA. Female G5PR^{Tg} mice showed higher levels of anti-dsDNA Ab than did female WT littermates (Fig. 5F). Female, but not male, G5PR^{Tg} mice also produced anti-nuclear Abs (Fig. 5G). Moreover, immunohistochemical staining of the kidneys of aged female G5PR^{Tg} mice showed stronger signals for immune complexes with IgG and C3 in glomeruli than were observed in WT mice (Fig. 5H). Male G5PR^{Tg} mice did not show such autoantibody production, suggesting that generation of B-1a cells in G5PR^{Tg} mice is affected by factors including sex hormone (or hormones) and aging, as has been previously described for B-1 cells from New Zealand Black (NZB) mice (29).

We next measured *g5pr* transcripts and cell survival potential of B-1a cells from NZB mice by qRT-PCR. B-1a cells from aged female NZB mice showed higher levels of *g5pr* transcription than did B-2 cells of NZB mice (Fig. 6A). The B-1a cells were more resistant to BCR-mediated AICD in vitro than were the B-2 cells (Fig. 6B), which correlated with lower levels of JNK activation upon BCR crosslinking in the B-1a cells (Fig. 6C).

Taken together, our results show that G5PR is a critical factor for selection of peripheral B cells during the physiological immune response, and abnormal G5PR upregulation is associated with the development of autoimmunity.

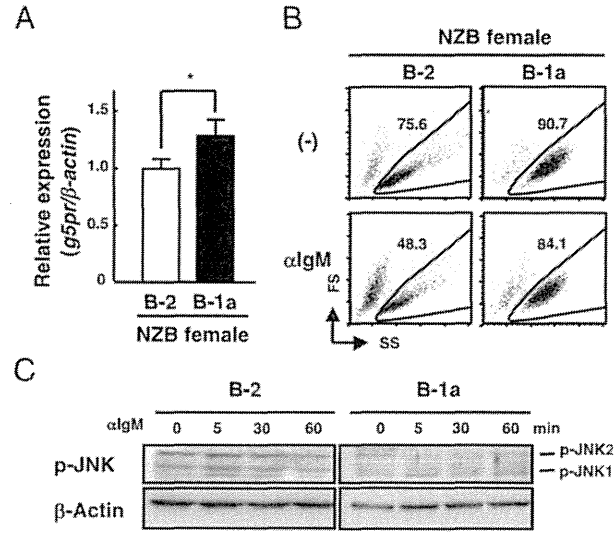

FIGURE 6. AICD and JNK phosphorylation in B cells of female NZB mice. (**A**) Expression of *g5pr* transcripts in B-1a or B-2 cells of NZB mice. Peritoneal B-1a or splenic B-2 cells were isolated from female NZB mice (n = 3), and *g5pr* expression was measured by qRT-PCR. Results are shown as the mean ± SD. *$p < 0.05$. (**B**) Survival of stimulated B-1a and B-2 cells. B-1a and B-2 cells from NZB mice were stimulated with αIgM for 24 h. Live cells were identified by forward scatter (FS) and side scatter (SS) signals on the flow cytometric profile. Results are representative of three independent experiments. (**C**) Activation of JNK in B-1a and B-2 cells of NZB mice. B-1a or B-2 cells were stimulated with αIgM for the indicated times. JNK phosphorylation was assessed by Western blotting. Results are representative of two independent experiments.

Discussion

G5PR is upregulated in mature GC B cells with $B220^{+}Fas^{+}GL7^{+}$ phenotype during normal immune responses to TD-Ags. These $G5PR^{high}$ B cells are selectively found at the centrocyte area of GCs. Centroblasts expressing Ki67, a marker of high proliferation potential (6), do not show G5PR upregulation. G5PR upregulation occurs in those B cells that have undergone class switching to IgG in the follicular region and appears in the $Ki67^{-}$ region. In addition, $G5PR^{high}$ B cells closely adhere to $CD35^{+}$ FDCs in GCs. These results indicate that G5PR is upregulated markedly in the centrocytes of GCs and can be used as a centrocyte marker in combination with Ki67, the marker for centroblasts. G5PR upregulation was induced by αIgM stimulation but was further augmented by αCD40 in vitro, suggesting that G5PR upregulation is reinforced by the interaction of B cells with FDCs and T_{FH} cells in GCs.

G5PR upregulation in centrocytes suggested to us that G5PR may have a cell stage-associated role in the regulation of BCR-mediated AICD for the selection of Ag-reactive GC B cells. Our results from transfecting WEHI-231 cells with a G5PR-overexpressing construct indicate that G5PR upregulation enhances B cell survival by inhibiting JNK phosphorylation. Unlike the case with transformed cells, young $G5PR^{Tg}$ mice did not show marked changes in the number and differentiation of B-lineage cells, and overexpression of G5PR did not cause any significant changes in B cell survival compared with that in WT mice under nonimmunized conditions in vivo or after αIgM stimulation of the Tg B cells in vitro.

We investigated whether the effect of G5PR upregulation appears during immune responses or is limited to the later response of BCR-mediated AICD. Upon immunization with TD-Ags, $G5PR^{Tg}$ mice indeed showed an increase in mature GC B cells, but this was characterized by more low-affinity or non-Ag–binding B cells than were seen in WT mice. The induction of T_{FH} cells was not affected in the spleens of Ag-immunized $G5PR^{Tg}$ mice. These findings suggest that the alteration of G5PR expression in GC B cells regulates BCR-mediated signals that might ultimately determine the threshold of high-affinity B cell selection in GCs.

Aged female $G5PR^{Tg}$ mice displayed a marked increase in B-1a cells with resistance to AICD in the peritoneal cavity. It is possible that this resistance is related to altered signal thresholds for cell survival or apoptosis. Many studies have compared BCR-mediated signaling between B-1 and B-2 cells of various mutant mice. CD19-Tg mice display more B-1 cells and autoimmune phenotype (30). B-1 cells show constitutive activation of ERK and NF-AT, and induced the high level of ERK signaling, but not activation of p38 and NF-κB or delayed JNK activation after αIgM stimulation (31). Btk-deficient mice exhibit a severe defect in B-1 cells (32). Further, the Src family tyrosine kinase Lyn is expressed in B-1 cells and is also involved in the hyporesponsive phenotype of B-1 cells (33). These observations suggest that B-1 cells depend more critically on BCR signaling than do B-2 cells in the peripheral lymphoid organs.

In comparison with G5PR-deficient B cells (22), increased G5PR expression reversely affected the JNK pathway leading to BCR-mediated AICD. However, G5PR overexpression resulted in only modest differences in the initial activation of JNK and Bim phosphorylation in B-1a cells. In fact, JNK activation was mildly reduced in peritoneal B-1a cells from aged female $G5PR^{Tg}$ mice at 60 min after αIgM stimulation, and this suppression of JNK activation was sustained. These results are in accordance with previous observations that prolonged JNK activation mediates the signal for apoptosis (34). Importantly, G5PR overexpression markedly reduced the level of c-Jun activation induced by αIgM stimulation, suggesting that the effect of G5PR overexpression was exerted predominantly via suppression of c-Jun target molecules. This idea may explain why $G5PR^{Tg}$ mice show only a mild phenotype with increased survival of B-1a cells, whereas the survival of B-2 cells of G5PR-deficient mice is severely impaired (22).

B-1 cells of autoimmune-prone mice are resistant to BCR-mediated AICD in vitro (35). A number of studies have attempted to elucidate the molecular mechanism regarding this B-1 cell–specific resistance to apoptosis (31, 36). Our results show that an increased expression of the *g5pr* gene does not affect the proliferation of B-1a cells in response to LPS stimulation but is associated with increased resistance to BCR-mediated AICD in B-1a cells, which might be associated with the generation of autoantibodies and autoimmunity. Overexpression of the *g5pr* gene did not cause abnormalities in the cell number and maturation of B cells in young $G5PR^{Tg}$ mice, suggesting that the increase in *g5pr* transcription might be within a level that can maintain normal proportions of B-1a, B-1b, and B-2 cells in mice. B-1a cells, however, became resistant to BCR-mediated AICD and increased in the peritoneal cavity in aged female $G5PR^{Tg}$ mice, suggesting that the effect of G5PR upon BCR-mediated signaling is regulated by the age and gender. The endogenous *G5PR* gene is located on chromosome 12 in mice, and the *G5PR* Tg is not linked to the X chromosome, as the $G5PR^{Tg}$ mouse colony is maintained by backcrossing male $G5PR^{Tg}$ mice with female WT mice.

Our results provide novel insights into the mechanism of B cell selection in GCs in peripheral lymphoid organs during immune responses to TD-Ags and into the generation of abnormal autoreactive B cell clones during aging. These findings suggest that investigating regulation of *g5pr* transcription might help further our understanding of the risk factors, onset, and molecular mechanisms involved in development of autoimmunity, potentially also assisting in the design of treatment for autoimmune diseases.

Acknowledgments

We thank M. Ito and Y. Fukushima for assistance.

Disclosures

The authors have no financial conflicts of interest.

References

1. MacLennan, I. C. 1994. Germinal centers. *Annu. Rev. Immunol.* 12: 117–139.
2. Rajewsky, K. 1996. Clonal selection and learning in the antibody system. *Nature* 381: 751–758.
3. Liu, Y. J., and C. Arpin. 1997. Germinal center development. *Immunol. Rev.* 156: 111–126.
4. Liu, Y. J., J. Zhang, P. J. Lane, E. Y. Chan, and I. C. MacLennan. 1991. Sites of specific B cell activation in primary and secondary responses to T cell-dependent and T cell-independent antigens. *Eur. J. Immunol.* 21: 2951–2962.
5. Han, S., B. Zheng, Y. Takahashi, and G. Kelsoe. 1997. Distinctive characteristics of germinal center B cells. *Semin. Immunol.* 9: 255–260.
6. Carter, R. H., and R. Myers. 2008. Germinal center structure and function: lessons from CD19. *Semin. Immunol.* 20: 43–48.
7. Tew, J. G., M. H. Kosco, G. F. Burton, and A. K. Szakal. 1990. Follicular dendritic cells as accessory cells. *Immunol. Rev.* 117: 185–211.
8. Vinuesa, C. G., M. A. Linterman, C. C. Goodnow, and K. L. Randall. 2010. T cells and follicular dendritic cells in germinal center B-cell formation and selection. *Immunol. Rev.* 237: 72–89.
9. Kurosaki, T. 2000. Functional dissection of BCR signaling pathways. *Curr. Opin. Immunol.* 12: 276–281.
10. Niiro, H., and E. A. Clark. 2002. Regulation of B-cell fate by antigen-receptor signals. *Nat. Rev. Immunol.* 2: 945–956.
11. Niiro, H., A. Maeda, T. Kurosaki, and E. A. Clark. 2002. The B lymphocyte adaptor molecule of 32 kD (Bam32) regulates B cell antigen receptor signaling and cell survival. *J. Exp. Med.* 195: 143–149.
12. Dal Porto, J. M., S. B. Gauld, K. T. Merrell, D. Mills, A. E. Pugh-Bernard, and J. Cambier. 2004. B cell antigen receptor signaling 101. *Mol. Immunol.* 41: 599–613.

13. Richards, J. D., S. H. Davé, C. H. Chou, A. A. Mamchak, and A. L. DeFranco. 2001. Inhibition of the MEK/ERK signaling pathway blocks a subset of B cell responses to antigen. *J. Immunol.* 166: 3855–3864.
14. Piatelli, M. J., C. Doughty, and T. C. Chiles. 2002. Requirement for a hsp90 chaperone-dependent MEK1/2-ERK pathway for B cell antigen receptor-induced cyclin D2 expression in mature B lymphocytes. *J. Biol. Chem.* 277: 12144–12150.
15. Graves, J. D., K. E. Draves, A. Craxton, J. Saklatvala, E. G. Krebs, and E. A. Clark. 1996. Involvement of stress-activated protein kinase and p38 mitogen-activated protein kinase in mIgM-induced apoptosis of human B lymphocytes. *Proc. Natl. Acad. Sci. USA* 93: 13814–13818.
16. Swart, J. M., D. M. Bergeron, and T. C. Chiles. 2000. Identification of a membrane Ig-induced p38 mitogen-activated protein kinase module that regulates cAMP response element binding protein phosphorylation and transcriptional activation in CH31 B cell lymphomas. *J. Immunol.* 164: 2311–2319.
17. Takada, E., K. Hata, and J. Mizuguchi. 2006. Requirement for JNK-dependent upregulation of BimL in anti-IgM-induced apoptosis in murine B lymphoma cell lines WEHI-231 and CH31. *Exp. Cell Res.* 312: 3728–3738.
18. Healy, J. I., R. E. Dolmetsch, L. A. Timmerman, J. G. Cyster, M. L. Thomas, G. R. Crabtree, R. S. Lewis, and C. C. Goodnow. 1997. Different nuclear signals are activated by the B cell receptor during positive versus negative signaling. *Immunity* 6: 419–428.
19. Healy, J. I., and C. C. Goodnow. 1998. Positive versus negative signaling by lymphocyte antigen receptors. *Annu. Rev. Immunol.* 16: 645–670.
20. Kurosaki, T. 2002. Regulation of B cell fates by BCR signaling components. *Curr. Opin. Immunol.* 14: 341–347.
21. Grimaldi, C. M., R. Hicks, and B. Diamond. 2005. B cell selection and susceptibility to autoimmunity. *J. Immunol.* 174: 1775–1781.
22. Xing, Y., H. Igarashi, X. Wang, and N. Sakaguchi. 2005. Protein phosphatase subunit G5PR is needed for inhibition of B cell receptor-induced apoptosis. *J. Exp. Med.* 202: 707–719.
23. Huq Ronny, F. M., H. Igarashi, and N. Sakaguchi. 2006. BCR-crosslinking induces a transcription of protein phosphatase component G5PR that is required for mature B-cell survival. *Biochem. Biophys. Res. Commun.* 340: 338–346.
24. Kono, Y., K. Maeda, K. Kuwahara, H. Yamamoto, E. Miyamoto, K. Yonezawa, K. Takagi, and N. Sakaguchi. 2002. MCM3-binding GANP DNA-primase is associated with a novel phosphatase component G5PR. *Genes Cells* 7: 821–834.
25. Iritani, B. M., K. A. Forbush, M. A. Farrar, and R. M. Perlmutter. 1997. Control of B cell development by Ras-mediated activation of Raf. *EMBO J.* 16: 7019–7031.
26. Sakaguchi, N., T. Kimura, S. Matsushita, S. Fujimura, J. Shibata, M. Araki, T. Sakamoto, C. Minoda, and K. Kuwahara. 2005. Generation of high-affinity antibody against T cell-dependent antigen in the Ganp gene-transgenic mouse. *J. Immunol.* 174: 4485–4494.
27. Toda, T., M. Kitabatake, H. Igarashi, and N. Sakaguchi. 2009. The immature B-cell subpopulation with low RAG1 expression is increased in the autoimmune New Zealand Black mouse. *Eur. J. Immunol.* 39: 600–611.
28. Rothstein, T. L., and D. L. Kolber. 1988. Anti-Ig antibody inhibits the phorbol ester-induced stimulation of peritoneal B cells. *J. Immunol.* 141: 4089–4093.
29. Shirai, T., T. Okada, and S. Hirose. 1992. Genetic regulation of CD5+ B cells in autoimmune disease and in chronic lymphocytic leukemia. *Ann. N. Y. Acad. Sci.* 651: 509–526.
30. Sato, S., N. Ono, D. A. Steeber, D. S. Pisetsky, and T. F. Tedder. 1996. CD19 regulates B lymphocyte signaling thresholds critical for the development of B-1 lineage cells and autoimmunity. *J. Immunol.* 157: 4371–4378.
31. Wong, S. C., W. K. Chew, J. E. Tan, A. J. Melendez, F. Francis, and K. P. Lam. 2002. Peritoneal CD5+ B-1 cells have signaling properties similar to tolerant B cells. *J. Biol. Chem.* 277: 30707–30715.
32. Khan, W. N., F. W. Alt, R. M. Gerstein, B. A. Malynn, I. Larsson, G. Rathbun, L. Davidson, S. Müller, A. B. Kantor, L. A. Herzenberg, et al. 1995. Defective B cell development and function in Btk-deficient mice. *Immunity* 3: 283–299.
33. Chan, V. W., F. Meng, P. Soriano, A. L. DeFranco, and C. A. Lowell. 1997. Characterization of the B lymphocyte populations in Lyn-deficient mice and the role of Lyn in signal initiation and down-regulation. *Immunity* 7: 69–81.
34. Liu, J., and A. Lin. 2005. Role of JNK activation in apoptosis: a double-edged sword. *Cell Res.* 15: 36–42.
35. Tsubata, T., M. Murakami, and T. Honjo. 1994. Antigen-receptor cross-linking induces peritoneal B-cell apoptosis in normal but not autoimmunity-prone mice. *Curr. Biol.* 4: 8–17.
36. Bikah, G., J. Carey, J. R. Ciallella, A. Tarakhovsky, and S. Bondada. 1996. CD5-mediated negative regulation of antigen receptor-induced growth signals in B-1 B cells. *Science* 274: 1906–1909.

European Journal of Immunology

Phenotype conversion from rheumatoid arthritis to systemic lupus erythematosus by introduction of *Yaa* mutation into FcγRIIB-deficient C57BL/6 mice

Shinya Kawano[*1], *Qingshun Lin*[*2], *Hirofumi Amano*[1], *Toshiyuki Kaneko*[1], *Keiko Nishikawa*[2], *Hiromichi Tsurui*[2], *Norihiro Tada*[3], *Hiroyuki Nishimura*[4], *Toshiyuki Takai*[5], *Toshikazu Shirai*[2], *Yoshinari Takasaki*[1] *and Sachiko Hirose*[2]

[1] Department of Internal Medicine, Juntendo University School of Medicine, Tokyo, Japan
[2] Department of Pathology, Juntendo University School of Medicine, Tokyo, Japan
[3] Atopy Research Center, Juntendo University School of Medicine, Tokyo, Japan
[4] Toin Human Science and Technology Center, Department of Biomedical Engineering, Toin University of Yokohama, Yokohama, Japan
[5] Department of Experimental Immunology and CREST of JST, Institute of Development, Aging and Cancer, Tohoku University, Sendai, Japan

We previously established an IgG Fc receptor IIB (FcγRIIB)-deficient C57BL/6 (B6)-congenic mouse strain (KO1), which spontaneously develops rheumatoid arthritis (RA), but not systemic lupus erythematosus (SLE). Here, we show that when Y chromosome-linked autoimmune acceleration (*Yaa*) mutation was introduced in KO1 strain (KO1.*Yaa*), the majority of KO1.*Yaa* mice did not develop RA, but instead did develop SLE. This phenotype conversion did not depend on autoantibody specificity, since KO1.*Yaa* mice, compared with KO1, showed a marked increase in serum levels of both lupus-related and RA-related autoantibodies. The increase in frequencies of $CD69^+$ activated B cells and T cells, and the spontaneous splenic GC formation with T follicular helper cell generation were manifest early in life of KO1.*Yaa*, but not KO1 and B6.*Yaa*, mice. Activated $CD4^+$ T cells from KO1.*Yaa* mice showed upregulated production of IL-21 and IL-10, compared with the finding in KO1 mice, indicating the possibility that this aberrant cytokine milieu relates to the disease phenotype conversion. Thus, our model is useful to clarify the shared and the disease-specific mechanisms underlying the clinically distinct systemic autoimmune diseases RA and SLE.

Keywords: Cytokines · FcγRIIB receptor · Rheumatoid arthritis · Systemic lupus erythematosus · *Yaa* mutation

Introduction

IgG Fc receptor IIB (FcγRIIB) is a major negative regulator of BCR-mediated activation signals in B cells [1]. We previously found that the *Fcgr2b* gene encoding FcγRIIB is polymorphic, and that autoimmune disease-prone mouse strains, such as NZB, BXSB, MRL, and NOD, all share deletion polymorphism in the AP-4-binding site in the *Fcgr2b* promoter region [2]. Because of the

Correspondence: Prof. Sachiko Hirose
e-mail: sacchi@juntendo.ac.jp

*These authors contributed equally to this work.

defective AP-4 binding, mice with this autoimmune-type allele polymorphism show downregulation of FcγRIIB expression levels in activated GC B cells, resulting in upregulation of IgG autoantibody production [3, 4]. These observations suggested that the autoimmune-type *Fcgr2b* confers the basis of susceptibility to autoimmune diseases. Consistent was our earlier finding that systemic lupus erythematosus (SLE) phenotypes in BXSB male mice carrying Y chromosome-linked autoimmune acceleration (*Yaa*) mutation were almost completely inhibited by the substitution of the autoimmune-type *Fcgr2b* for the wild C57BL/6 (B6)-type *Fcgr2b* [5]. However, because BXSB female mice carrying the autoimmune-type *Fcgr2b* but lacking *Yaa* did not develop SLE, it is likely that the autoimmune-type *Fcgr2b* contributes to SLE susceptibility through a strong epistatic interaction with *Yaa* mutation.

To examine further the role of the downregulated expression of FcγRIIB in autoimmune diseases, we recently established an FcγRIIB-deficient B6 mouse strain, KO1, by gene targeting in 129-derived embrionic stem cells and selective backcrossing to a B6 background. Intriguingly, KO1 did not develop SLE, but instead developed severe rheumatoid arthritis (RA), as reported previously [6]. This KO1 strain carried a 129-derived approximately 6.3 Mb interval distal from the null-mutated *Fcgr2b* gene within the *Sle16* locus, which is shown to induce loss of self-tolerance in the B6 background [7]. Boross et al. [8] reported that FcγRIIB-deficient B6 mice generated by gene targeting in B6-derived embryonic stem cells, thus lacking the 129-derived flanking *Sle16* locus, fail to develop any sign of autoimmune diseases. Thus, the development of RA in KO1 mice may be due to the epistatic interaction of FcγRIIB deficiency and *Sle16* locus.

Boross et al. [8] also reported that their FcγRIIB-deficient B6 mice develop lethal lupus nephritis in the presence of *Yaa* mutation, indicating the epistatsis between FcγRIIB-deficiency and *Yaa* in the development of full-blown autoimmune diseases. In addition, Subramanian et al. [9] reported that the strong epistatic interaction between *Yaa* and *Sle1*, which contains the autoimmune-predisposing *Slam/Cd2* haplotype, contributes to severe lupus nephritis. The *Sle16* locus also contains this autoimmune-predisposing *Slam/Cd2* haplotype [10].

In contrast to the accelerated effect of *Yaa* on lupus nephritis, Jansson and Holmdahl [11] reported the suppressive effect of *Yaa* on collagen-induced arthritis. In the present study, we have introduced *Yaa* mutation into FcγRIIB-deficient RA-prone KO1 mice to examine how *Yaa* affects the disease phenotypes in these mice. We found that the majority of KO1.*Yaa* mice did not develop RA, but instead did develop severe SLE early in life, and that this phenotype conversion did not depend on the shift of autoantibody specificity from RA-related to lupus-related one.

Characteristic clinical features differ between RA and SLE; however, both diseases share aberrant activation of immune processes associated with the production of a variety of autoantibodies and subsequent immune complex-mediated tissue inflammation. Our model is useful to investigate the shared and the disease-specific factors contributing to the clinically distinct systemic autoimmune diseases RA and SLE.

Results

Disease phenotype in Yaa-carrying FcγRIIB-deficient KO1 mice

KO1 mice developed arthritis after 4 months of age and the disease incidence and severity were increased with age. At 8 months of age, 67% of KO1 mice showed arthritis with marked swelling and stiffness of forepaws and hindpaws. In contrast, the incidence and severity of arthritis were markedly suppressed in KO1.*Yaa* mice and 88% of KO1.*Yaa* mice were free from arthritis (Fig. 1A). Representative macroscopic findings of forepaws and hindpaws of KO1 and KO1.*Yaa* mice at 8 months of age are shown in Figure 1B. Intriguingly, KO1 strain did not develop proteinuria; however, KO1.*Yaa* began to be positive for proteinuria at 2 months of age and the incidence of positive proteinuria reached 63% (Fig. 1C) with 46% mortality rate at 8 months of age (Fig. 1D).

Figure 1E shows a comparison of representative histopathological and immunofluorescent findings of renal glomeruli among B6, B6.*Yaa*, KO1, and KO1.*Yaa* mice at 4 months of age. In KO1.*Yaa* mice, glomeruli were significantly enlarged even at 4 months of age (Fig. 1F), because of a marked cellular proliferation in glomeruli and a large amount of IgG deposition in mesangial area and along glomerular capillary walls. These glomerular lesions were seldom observed in B6, B6.*Yaa*, and KO1 mice even at 8 months of age.

Serum levels of autoantibodies

To examine the relationship between the disease phenotype conversion from RA to SLE and the specificity of autoantibodies, we compared serum levels of lupus-related autoantibodies against dsDNA, chromatin, and RNP, and RA-related rheumatoid factor (RF), anti-type II collagen (CII), and -cyclic citrullinated peptide (CCP) antibodies at 2 and 6 months of age among B6, B6.*Yaa*, KO1, and KO1.*Yaa* mice (Fig. 2). KO1.*Yaa* mice showed higher serum levels of both lupus-related and RA-related autoantibodies than the other three strains of mice even at 2 months of age. The levels of all these antibodies were increased with age in KO1.*Yaa* mice. Age-associated increase was also observed in KO1 mice; however, the levels were remarkably higher in KO1.*Yaa* mice than those in KO1 mice at 6 months of age. Thus, the conversion of disease phenotype from RA to SLE was not explained by the shift of antibody specificity from RA-type to lupus-type.

Splenomegaly, subpopulation, and maturation/activation status of splenic lymphocytes

The spleen weight in B6, B6.*Yaa*, KO1, and KO1.*Yaa* mice was compared at 4 months of age. Splenomegaly was only observed in KO1.*Yaa* mice (Fig. 3A). Consistently, spontaneous GC formation was observed only in KO1.*Yaa* mice at 4 months of age (Fig. 3B).

Flow cytometric analysis of spleen cells from 4-month-old mice revealed that, while there were no differences in

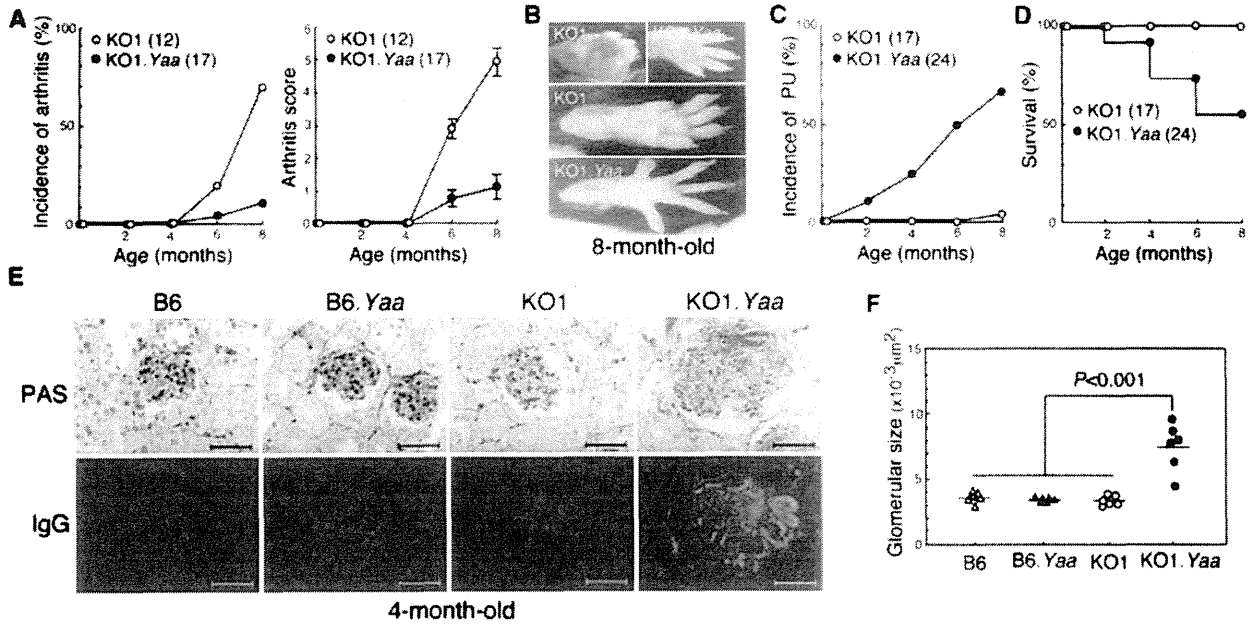

Figure 1. Disease phenotype shift from RA to SLE in KO1.*Yaa* mice. (A) Comparison of the cumulative incidence and score of arthritis between KO1 and KO1.*Yaa* mice. Score is shown as mean ± SE. (B) Representative macroscopic findings of forepaws and hindpaws in KO1 and KO1.*Yaa* mice at 8 months of age. The former mice show marked swelling and stiffness of the wrist and ankle joints. (C) Comparison of the cumulative incidence of proteinuria (PU) between KO1 and KO1.*Yaa* mice. (D) Comparison of survival rate between KO1 and KO1.*Yaa* mice. (E) Histopathological findings of glomeruli in B6, B6.*Yaa*, KO1, and KO1.*Yaa* at 4 months of age. Formalin-fixed sections were stained with periodic acid-Schiff/hematoxylin (PAS) (top). Frozen sections were stained with anti-mouse IgG (bottom) to evaluate the deposition of IgG in renal glomeruli. Scale bars = 50 μm. Representative results obtained from six mice in each strain. (F) Comparison of glomerular size as an indicator of the severity of glomerular lesion. The horizontal bar represents the mean. (A–F) All data are shown as the mean of the indicate numbers of mice in each panel and are representative of three experiments performed. Statistical significance was determined by Mann–Whitney's *U* test.

frequencies of $B220^+$ B cells per total spleen cells among four strains of mice (Table 1), there was a significant decrease in frequencies of $CD21^+CD23^-$ marginal zone B cells in *Yaa*-bearing B6.*Yaa* and KO1.*Yaa* mice (Fig. 4A and Table 1). This decrease is thought to be due to the effect of *Yaa* mutation, as reported previously [12], and not directly related to SLE phenotype. As for the activation/maturation status of B cells, frequencies of $CD69^+$ activated B cells, peanut agglutinin $(PNA)^+$ GC B cells, and $CD138^+$ plasma cells were significantly higher in KO1.*Yaa* mice than those found in other strains of mice (Fig. 4B and Table 1). As for T cells, while total $CD3^+$ T cells per total cells was significantly decreased in KO1.*Yaa* mice, the frequency of $CD69^+$ activated

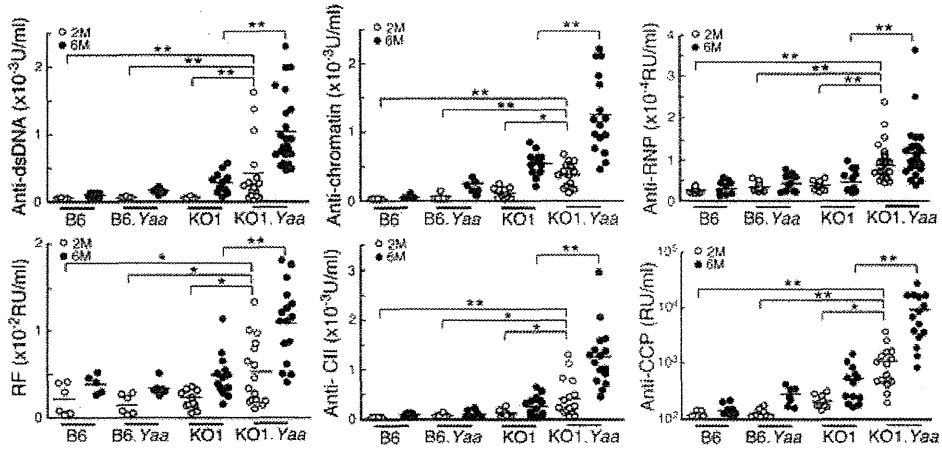

Figure 2. Comparisons of serum levels of lupus-related IgG autoantibodies against dsDNA, chromatin, and RNP, and RA-related IgG RF, anti-CII and -CCP antibodies among B6, B6.*Yaa*, KO1, and KO1.*Yaa* mice at 2 and 6 months of age. Each symbol represents an individual mouse and the bar represents the mean. Data shown are representative of three experiments performed. Statistical significance was determined by Mann–Whitney's *U* test (**$p < 0.001$, *$p < 0.05$).

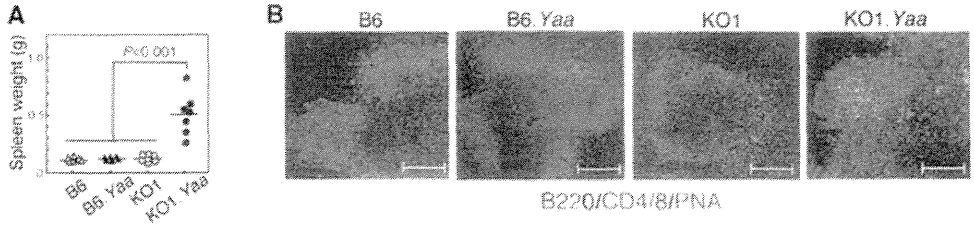

Figure 3. Splenomegaly with spontaneous GC formation in KO1.*Yaa* mice. (A) Comparison of spleen weight among B6, B6.*Yaa*, KO1, and KO1.*Yaa* mice at 4 months of age. Each symbol represents a single mouse and the bar represents the mean. Data shown are representative of three experiments performed. Statistical significance was determined by Mann–Whitney's *U* test. (B) Frozen spleen sections of 4-month-old mice were triple stained with a mixture of anti-CD4 and anti-CD8 mAbs (green), anti-B220 mAb (blue), and PNA (red) to examine the extent of GC formation. Representative results obtained from six mice in each strain are shown. Scale bar = 100 μm.

T cells was markedly increased in KO1.*Yaa* mice (Fig. 4C and Table 1). This activation of T cells may reflect the increases in the $CD4^+/CD8^+$ T-cell ratio and in the frequency of T_{FH} cells with $PD1^+ICOS^+CXCR5^+CD4^+$ phenotype (Fig. 4C and Table 1). Because the frequencies of $PD1^+ICOS^+CXCR5^+CD4^+$ T_{FH} cells in B6, B6.*Yaa*, and KO1 mice were within normal range (Table 1), the observed abnormal increase in $PD1^+ICOS^+CXCR5^+CD4^+$ T_{FH} cells in KO1.*Yaa* mice with overt SLE was thought to be due to the combined effect of the FcγRIIB-deficiency, *Sle16* locus, and *Yaa* mutation. Table 1 also shows that the frequency of $CD11b^+$ monocyte/macrophage population was significantly increased in KO1.*Yaa* mice with a comparable level observed in BXSB male mice [5].

Cytokine profile in spleen from KO1 and KO1.*Yaa* mice

To examine the difference in in vivo cytokine expression levels associated with phenotype conversion from RA to SLE, quantitative real-time PCR (qRT-PCR) analysis was performed to compare mRNA expression levels of notable cytokines in spleen between KO1 and KO1.*Yaa* mice at 4 months of age (Fig. 5A). The result showed that the expression of IL-6, IL-10, and IL-21 was significantly upregulated in KO1.*Yaa* mice compared with that in KO1 mice. Among these, the increase in IL-10 expression was prominent, with more than tenfold increase in KO1.*Yaa* mice. There was no significant difference in expression levels of other cytokines such as IL-2, IL-4, IL-17, IFN-γ, TNF-α, and IFN-α between two strains of mice.

We next examined the cellular source of IL-10 and IL-21, using flow cytometric analysis of PMA/ionomycin-stimulated spleen cells from 4-month-old KO1 and KO1.*Yaa* mice. Both IL-10 and IL-21 were secreted from $CD4^+$ T cells and the frequencies of IL-10 and IL-21-secreting cells per total $CD4^+$ T cells were significantly higher in KO1.*Yaa* than those in KO1 mice (mean ± SE of KO1 versus KO1.*Yaa*; IL-10: 7.56 ± 1.25 versus 14.74 ± 0.43, $p < 0.01$, IL-21: 5.09 ± 0.22 versus 9.91 ± 0.60, $p < 0.01$) (Fig. 5B), consistent with the results of qRT-PCR analysis. PD1 and ICOS expression levels were upregulated in in vitro stimulated $CD4^+$ T cells. Most IL-10 and IL-21-secreting cells showed high PD1 expression levels; however, the ICOS expression level was broadly distributed in these cytokine-secreting cells (Fig. 5B). As shown in Figure 5C, in addition to IL-10 and IL-21 single producers, the significant frequency of $CD4^+$ T cells secreted both cytokines.

Table 1. Subpopulations of splenocytes in KO1, KO1.*Yaa*, B6, and B6.*Yaa* mice at 4 months of age[a)]

	B6	B6.*Yaa*	KO1	KO1.*Yaa*
$B220^+$ B/total cells	50.5 ± 3.3	54.6 ± 3.4	53.5 ± 3.2	41.2 ± 5.7
$CD21^+CD23^-$ MZ B/total B	9.8 ± 0.8	2.7 ± 0.3[b)]	11.3 ± 1.2	2.3 ± 0.4[b)]
$CD69^+B220^+$ B/total B	2.7 ± 0.7	6.1 ± 1.8	2.3 ± 0.7	15.4 ± 2.8[c)]
PNA^+B220^+ B/total B	2.4 ± 0.2	2.4 ± 0.6	1.2 ± 0.1	8.1 ± 0.8[c)]
$CD138^+$ plasma/total cells	0.5 ± 0.0	1.0 ± 0.5	0.4 ± 0.1	2.6 ± 0.7[c)]
$CD3^+$ T/total cells	32.2 ± 1.6	27.9 ± 1.5	28.3 ± 2.1	18.8 ± 1.6[c)]
$CD69^+CD4^+$ T/total T	14.3 ± 2.1	19.3 ± 2.2	14.1 ± 1.3	44.6 ± 3.9[c)]
$CD4^+/CD8^+$ ratio	1.4 ± 0.1	1.6 ± 0.2	1.1 ± 0.1	6.1 ± 2.4[c)]
$CD25^+FoxP3^+CD4^+$ T/total T	18.0 ± 1.3	17.0 ± 1.3	16.0 ± 1.1	18.2 ± 0.2
$PD1^+ICOS^+CD4^+$ T/total T	2.6 ± 0.7	3.7 ± 1.2	2.1 ± 0.7	32.3 ± 3.4[c)]
$CXCR5^+PD1^+CD4^+$ T/total T	3.4 ± 0.8	3.7 ± 1.3	2.1 ± 0.7	13.2 ± 3.2[c)]
$CD11b^+$ cells/total cells	4.4 ± 0.5	4.7 ± 0.1	5.1 ± 0.2	13.3 ± 0.1[c)]

[a)] Results were obtained from six mice in each strain, and are shown as mean and SE.
[b)] The value is significantly different from B6 mice or KO1 mice ($p < 0.005$, Student's *t*-test).
[c)] The value is significantly different from other strains of mice ($p < 0.05$, Student's *t*-test).

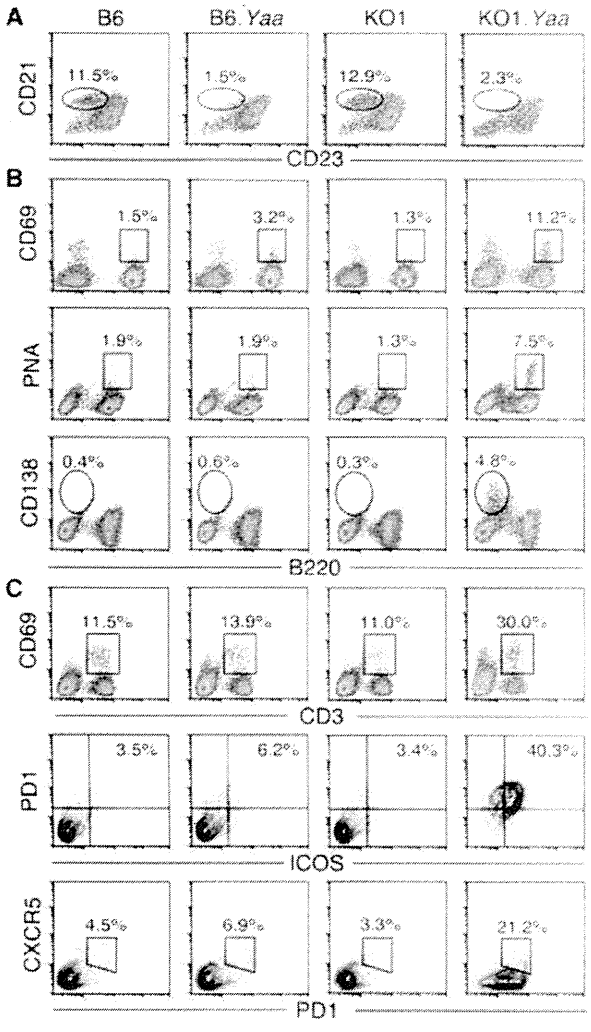

Figure 4. Comparisons of cell surface phenotypes of splenic lymphocytes among B6, B6.*Yaa*, KO1, and KO1.*Yaa* mice at 4 months of age, using flow cytometry. (A) Spleen cells were triple-stained with anti-B220, -CD21, and -CD23 mAbs, and CD21 and CD23 expression levels on $B220^+$ B cells were examined. The frequency of $CD21^+CD23^-$ marginal zone (MZ) B cells is shown. (B) Activation/maturation status of B cells. Spleen cells were stained with anti-CD69, -CD138, -B220 mAbs, and PNA. Frequencies of $CD69^+$ activated B cells per total B cells, PNA^+ GC B cells per total B cells, and $CD138^+$ plasma cells per total cells are shown. (C) Activation/maturation status of T cells. Spleen cells were stained with anti-CD69 and -CD3 mAbs, and the frequency of $CD69^+$ activated T cells per total $CD3^+$ T cells is shown. Cells were further stained with anti-CD4, -PD1, -ICOS, and -CXCR5 mAbs, and the frequencies of $PD1^+ICOS^+CD4^+$ and $PD1^+CXCR5^+CD4^+$ T_{FH} cells per total $CD4^+$ T cells are shown. Representative results obtained from six mice in each strain are shown.

Discussion

The current study showed that introduction of *Yaa* mutation into RA-prone KO1 mice leads to conversion of disease phenotypes from RA to SLE. RA and SLE are both classified as systemic autoimmune diseases. Since features of RA are occasionally associated with the clinical pictures of SLE [13], it has long been suggested that certain shared genetic pathways, as well as disease-specific ones, underlie the pathogenesis of both RA and SLE [14]. Our current model provided a clue to investigate this issue and suggested that, while the FcγRIIB deficiency and *Sle16* locus in KO1 genetic background confers predisposition to RA [6], an additional epistatic effect of *Yaa* mutation induces conversion of the disease phenotype from RA to SLE.

It has been shown that an etiology of *Yaa*-mediated B-cell activation is the duplication of the *Tlr7* gene [9,15,16]. The ligand for TLR7 is single-stranded RNA, thus suggesting that overexpression of TLR7 activates B cells by RNA-containing autoantigens, resulting in RNA-associated lupus autoantibody production. However, in the present study, *Yaa*-mediated disease phenotype conversion from RA to SLE was not explained by the shift of autoantibody specificity, and rather *Yaa*-mediated B-cell activation seems to be polyclonal in KO1.*Yaa* mice. This polyclonal B-cell activation may relate to the marked spontaneous GC formation and the T_{FH}-cell generation that developed in the spleen early in life of KO1.*Yaa* mice. The formation of GC depends on intrafollicular localization of antigen, activated B cells and T cells [17,18]. Among subsets of $CD4^+$ T cells, T_{FH} cells are the specialized subset to help B cells to generate affinity-matured antibodies [17]. In addition to the B-cell help by T_{FH} cells in GC reaction, it has been shown that the relationship between B cells and T_{FH} cells is a reciprocal dependency, and that the cognate interaction with activated B cells is required for the maintenance of $PD\text{-}1^+ICOS^+CXCR5^+$ T_{FH} cells [19]. This is consistent with the present study, in which the combined effect of FcγRIIB-deficiency, *Sle16* locus, and *Yaa* mutation accelerated not only spontaneous PNA^+ B-cell generation and GC formation but also T_{FH}-cell generation in KO1.*Yaa* mice. As this vicious cycle of activated B cells and T_{FH} cells promotes polyclonal B-cell activation, KO1.*Yaa* mice showed the marked increase in serum levels of both lupus-related and RA-related autoantibodies.

Anti-CCP antibodies are currently considered to be the most specific autoantibodies for RA patients, although some patients with SLE and Sjögren's syndrome were found to have these autoantibodies [20]. Anti-CCP antibodies react with citrullinated proteins, which are the product of posttranslational modification. Citrullination of protein is a physiological process and is catalyzed by peptidyl arginine deiminase enzymes. Anti-CCP antibodies may thus gain the arthritogenicity when citrullinated proteins are increased, particularly in the arthritic region [20]. In mouse models, an increased serum level of anti-CCP antibodies was observed in SLE-prone and arthritis-free *bcl-2*-transgenic (NZW × B6)F1 mice [21], as in the case of KO1.*Yaa* mice in the current study. Thus, it appears that this autoantibody specificity is not exclusively associated with inflammatory joint diseases.

In KO1.*Yaa* mice, there was a significant increase in the IL-21 expression level early in life compared with that in KO1 mice. IL-21 is a potent immunoregulatory cytokine produced by NKT cells and $CD4^+$ T cells, and it has recently been shown that IL-21 is an autocrine growth factor for T_{FH} cells [17,22]. Many cell types express the receptors for IL-21, but the level of expression on B cells is the highest and drives terminal differentiation of B cells and plasma cells [19,22]. Intriguingly, Bubier et al. [23]

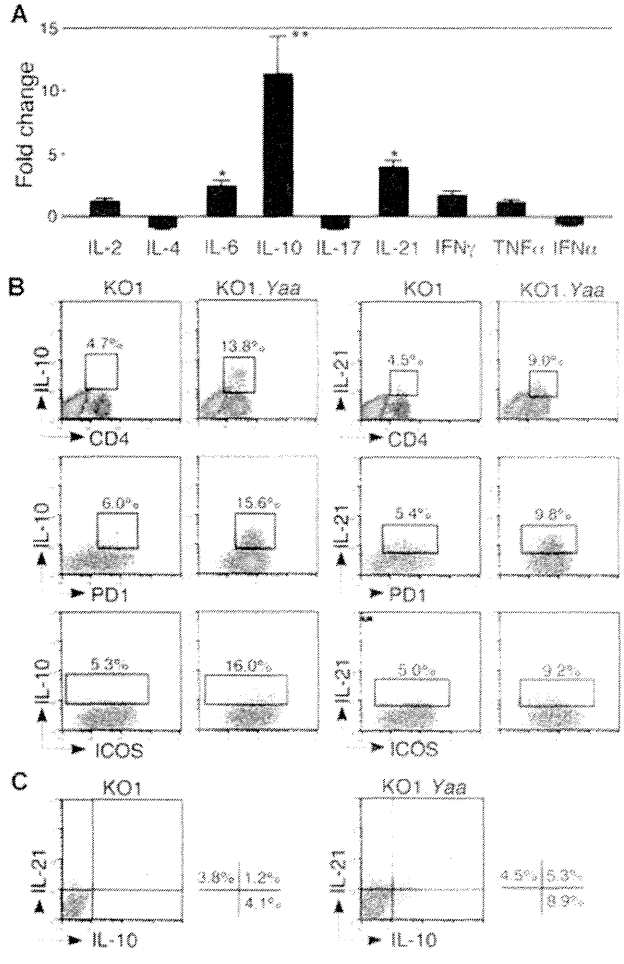

Figure 5. Comparisons of cytokine synthesis between KO1 and KO1.*Yaa* mice at 4 months of age. (A) Quantitative real-time PCR analysis of cytokine mRNA expression levels in spleen from KO1 and KO1.*Yaa* mice. Value of KO1 mice was designated as 1, and values of KO1.*Yaa* mice were evaluated as fold change compared with the values in KO1 mice. Data are shown as mean + SE of four mice for each strain and representative of three experiments performed. Statistical significance was determined by Mann–Whitney's *U* (*$p < 0.05$, **$p < 0.01$). (B) Flow cytometric analysis of IL-10 and IL-21-secreting cells in PMA/ionomycin-stimulated spleen cells from KO1 and KO1.*Yaa* mice. Frequencies of each cytokine secreting cells per total $CD4^+$ T cells, $CD4^+PD1^+$ T cells and $CD4^+ICOS^+$ T cells are shown. (C) Flow cytometric analysis of IL-10 and L-21-secreting cells, using gated $CD4^+$ T cells. Representative results obtained from six mice in each strain are shown.

reported that SLE phenotypes including autoantibody production in BXSB male mice were almost completely inhibited in the mice with the deficient IL-21 receptor. Furthermore, Rankin et al. [24] recently reported that IL-21 receptor-deficient MRL/*lpr* mice were devoid of abnormal systemic accumulation of activated B cells and T cells. These findings suggest that IL-21-mediated signals play an essential role for the pathogeneses of SLE.

It has been shown that IL-21 is a potent regulator of IL-10, since IL-10 production decreases in IL-21 receptor knockout mice, while it increases in IL-21-transgenic mice [25]. IL-10 was first described as a factor produced by Th2 cells, which inhibited the production of cytokines by Th1 cells [26]. Accumulating evidence, however, have shown that IL-10 is actually produced by many types of cells, and that, although IL-10 shows antiinflammatory properties against T cells and macrophages through inhibiting the production of inflammatory cytokines, it promotes B-cell function to induce antibody production [27, 28]. Considering these dual effects with immunosuppressive and immunostimulatory properties, IL-10 may confer different effects on the disease progression processes of RA and SLE. Indeed, the hallmark of RA is the excess production of inflammatory cytokines by T cells and macrophages at inflammatory foci, while SLE is characterized by increased production of high-affinity autoantibodies and deposition of their immune complexes in a wide variety of tissues, particularly in renal glomeruli. Consistently, there are several reports indicating the suppressive effect of IL-10 on RA [27, 29] and the promoting effect of IL-10 on lupus pathogenesis [30]. Further studies are needed to define the role of IL-10 in the conversion of disease phenotypes observed in the present study. These studies are underway in our laboratory.

Peripheral blood mononuclear cells from patients with active SLE show up-regulated expression of a group of type I IFN-induced genes [31–33]. Thus, IFN-α seems to be an important cytokine in SLE pathogenesis. In pristane-induced lupus model, the disease was shown to be associated with excess IFN-α production [34], as in the case of human SLE. However, overexpression of IFN-α is not likely to be involved in SLE pathogenesis in KO1.*Yaa* mice, since there were no differences in IFN-α expression levels between RA-prone KO1 mice and SLE-prone KO1.*Yaa* mice. Accumulating evidence shows that IL-6, IL-17, and TNF-α are important contributing cytokines to the pathogenesis of RA [35–37]. In the present studies, however, IL-6 expression levels were increased in SLE-prone KO1.*Yaa* mice compared with those in RA-prone KO1 mice, and there was no significant difference in expression levels of IL-17 and TNF-α between KO1 and KO1.*Yaa* mice. Thus, these cytokines are suggested to be unrelated to the observed phenotype conversion from RA to SLE in our model.

In conclusion, we introduced *Yaa* mutation into RA-prone KO1 strain and found that the disease phenotype converted from RA to SLE in KO1.*Yaa* mice. This phenotype conversion was likely to be due to the changes in cytokine milieus rather than the shift of autoantibody specificity from RA-related to lupus-related one. Further studies for the clarification and identification of the mechanism underlying this phenotype conversion are of paramount importance for shedding light on the mechanisms that control the development of clinically distinct systemic autoimmune diseases RA and SLE.

Materials and methods

Mice

FcγRIIB-deficient KO1 mice were generated by gene targeting in 129-derived embryonic stem cells and by backcrossing to B6 for over 12 generations [6]. The *Yaa* mutation was introduced into

KO1 mice by crossing with B6.*Yaa* mice. B6.*Yaa* mice were purchased from the Jackson Laboratory. All mice were housed under identical conditions. Experiments were performed in accordance with our institutional guidelines. Male mice were analyzed in the current study.

Incidence of arthritis

Ankle joint swelling was examined by inspection and arbitrarily scored as follows: 0, no swelling; 1, mild swelling; 2, moderated swelling; 3, severe swelling. Scores of both ankle joints are put together, and mice with scores over 2 were considered positive for arthritis.

Measurement of proteinuria

The proteinuria was monitored by biweekly testing and scored as previously descrobed [38]. Briefly, urine samples (10 μL) spotted on filter paper were air dried, fixed in 70% ethanol and stained with bromophenol blue solution. A series of standard three-fold dilution of BSA were processed as the same way, and the degree of proteinuria was assessed by visually comparing the color intensity of urine spot with that of the spot of BSA standards. Scores are as follows; 0:<37 mg/100 mL 1:≧37 mg/100 mL, 2:≧74 mg/mL, 3:≧111 mg/100 mL, 4:≧333 mg/100 mL, 5:≧1000 mg/100 mL, and 6:≧3000 mg/100 mL. Mice with urinary protein levels of four or more in repeated tests were considered as positive for proteinuria.

Histopathology and tissue immunofluorescence

Tissues fixed in 4% paraformaldehyde and embedded in paraffin were sectioned at 2 μm thickness, and tissue sections were stained with periodic acid-Schiff and hematoxylin (PAS). For immunofluorescence, tissues were embedded in Tissue-Tek OCT compound, frozen in liquid nitrogen, and sectined at 4 μm thickness. Frozen kidney sections were stained with FITC-labeled polyclonal goat anti-mouse IgG for 60 min at room temperature. For analysis of splenic tissues, frozen sections were three-color stained with Alexa 488-labeled anti-CD4 and -CD8 mAbs, Alexa 647-labeled anti-B220 mAb, and Alexa 546-labeled PNA. Antibodies and PNA were purchased from BD Pharmingen (San Diego, CA) and Vector Laboratories Inc. (Burlingame, CA), respectively. The labeling of these reagents was performed in our laboratory. Color images were obtained using laser scanning microscopy (Zeiss LSM510, Carl Zeiss Co., Ltd., Germany).

Estimation of the severity of glomerular lesion

The extent of cellular proliferation in glomerular lesion was estimated by the measurement of glomerular size. Kidney section stained by PAS was photographed under a microscope (Biozero, KEYENCE, Osaka, Japan) with ×50 magnification. Ten glomeruli in each field were randomly selected in order of size, and the size of each glomerulus was calculated using BZ-II analyzer software (KEYENCE). Mean size of 10 glomeruli was used as an indicator of histological severity of lupus nephritis in each individual mouse.

Serum levels of autoantibodies

Serum levels of IgG anti-dsDNA and -chromatin antibodies were measured using ELISA, as previously described [39]. Serum antibody levels are expressed in units, referring to a standard curve obtained by the serial dilution of a pooled serum of (NZB × NZW) F1 mice over 8 months, containing 1000 units/mL. Serum levels of IgG anti-RNP antibodies were measured by employing a commercially available kit (Alpha Diagnostic Intl. Inc., San Antonio, TX), and are expressed as relative units according to the manufacturer's instructions.

Serum levels of IgG RF and IgG anti-CCP antibodies were measured employing commercially available kits (Shibayagi Co. Ltd., Gunma, Japan and Cosmic Corporation, Tokyo, Japan, respectively), and are expressed as relative units according to the manufacturer's instructions. Serum levels of IgG anti-CII antibodies were measured using an ELISA plate precoated with bovine CII (Sigma-Aldrich, St. Louis, MO). CII-binding activities are expressed in units, referring to a standard curve obtained by serial dilution of a standard serum pool from KO1 mice hyper-immunized with CII, containing 1000 unit activities/mL.

Flow cytometric analysis

For the analysis of splenic lymphocytes, spleen cells were stained with the following reagents: FITC-conjugated anti-CD3, -CD21, -ICOS, -Foxp3, and -CD11b mAbs, Pacific blue-conjugated anti-B220, -CD4 mAbs, and PNA, PE-conjugated anti-B220, -CD138, -PD1, and -CD25 mAbs, and biotin-conjugated anti-CD69, -CD23, -CD8, and -CXCR5 mAbs, followed by streptavidin allophycocyanin. mAbs for CD25 and those for Foxp3, PD1, and ICOS were obtained from BioLegend (San Diego, CA) and eBioscience (San Diego, CA), respectively. Others were from BD PharMingen. Stained cells were four-color analyzed using a FACSAria cytometer and FlowJo software (Tree Star, Inc., Ashland, OR) with whole cell-gate excluding dead cells in forward and side scatter cytogram.

For intracellular cytokine staining of spleen cells, cells were stimulated with PMA (0.2 μg/mL)/ionomycin (2 μg/mL) in the presence of Golgi-Stop (BD Bioscience, San Jose, CA) for 5 h and stained with Pacific Blue-labeled anti-CD4 and biotin-labeled anti-PD1 or anti-ICOS mAbs followed by streptavidine allophycocyanin. Stained cells were then fixed and permeabilized using BD Cytofix/Cytoperm (BD Bioscience), followed by staining with FITC-labeled anti-IL-10, and PE-labeled anti-IL-21 mAbs. Stained cells were analyzed as above.

qRT-PCR analysis

Total RNA was isolated from spleen and first-stranded cDNA was synthesized using an oligo(dT)-primer with Superscript II First-Strand Synthesis kit (Invitrogen, Carlsbad, CA). The cDNA product was used for each qRT-PCR sample. The data were normalized to β-actin reference. Primer pairs used were as follows: IL-2 (forward) 5′-AACCTGAAACTCCCCAGGAT-3′, (reverse) 5′-AGGGCTT GTTGAGATGATGC-3′; IL-4 (forward) 5′-CCTCACAGCAACGAA GAACA-3′, (reverse) 5′-AAGTTAAAGCATGGTGGCTCA-3′; IL-6 (forward) 5′-GACAAAGCCAGAGTCCTTCAGAGAG-3′, (reverse) 5′-CTAGGTTTGCCGAGTAGATCTC-3′; IL-10 (forward) 5′-CCAA GCCTTATCGGAAATGA-3′, (reverse) 5′-TGGCCTTGTAGACACCT TGG-3′; IL-17 (forward) 5′-TCTCTGATGCTGTTGCTGCT-3′, (reverse) 5′-GACCAGGATCTCTTGCTGGA-3′; IL-21 (forward) 5′-ATCCTGAACTTCTATCAGCTCCAC-3′, (reverse) 5′-GCATTTAGCT ATGTGCTTCTGTTTC-3′; IFNγ (forward) 5′-AAGACAATCAGGCC ATCAGC-3′, (reverse) 5′-ATCAGCAGCGACTCCTTTTC-3′; TNF-α (forward) 5′-GGCAGGTCTACTTTGGAGTCATTGC-3′, (reverse) 5′-ACATTCGAGGCTGCTCCAGTGAATTCGG-3′; consensus IFNα (forward) 5′-ATGGCTAGRCTCTGTGCTTTCCT-3′, (reverse) 5′-AG GGCTCTCCAGAYTTCTGCTCTG-3′; β-actin (forward) 5′-AGCCAT GTACGTAGCCATCC-3′, and (reverse) 5′-CTCTCAGCTGTGGTGG TGAA-3′. The quantity was normalized using the formula of the $2^{-\Delta\Delta CT}$ method.

Statistical analysis

Statistical analysis was performed using Mann–Whitney's *U* test for disease phenotypes and Student's *t*-test for flow cytometric analysis. A value of $p < 0.05$ was considered as statistically significant.

Acknowledgments: The authors thank Dr. A. Sato-Hayashizaki, Mr. N. Ishihara, Ms. K. Kojyo, Ms. N. Ohtsuji, and Ms. T. Ikegami for excellent technical assistance. This work was supported in part by Grants-in-Aid for Scientific Research (C) from the Ministry of Education, Science, Technology, Sports and Culture of Japan, and Grant for Research on Intractable Diseases from the Ministry of Health, Labour, and Welfare of Japan.

Conflict of interest: The authors declare no financial or commercial conflict of interest.

References

1 Ravetch, J. V. and Kinet, J.-P., Fc receptors. *Annu. Rev. Immunol.* 1991. 9: 457–492.

2 Jiang, Y., Hirose, S., Abe, M., Sanokawa-Akakura, R., Ohtsuji, M., Mi, X., Li, N. et al., Polymorphisms in IgG Fc receptor IIB regulatory regions associated with autoimmune susceptibility. *Immunogenetics* 2000. 51: 429–435.

3 Jiang, Y., Hirose, S., Sanokawa-Akakura, R., Abe, M., Mi, X., Li, N., Miura, Y. et al., Genetically determined aberrant down-regulation of FcgRIIB1 in germinal center B cells associated with hyper-IgG and IgG autoantibodies in murine systemic lupus erythematosus. *Int. Immunol.* 1999. 11: 1685–1691.

4 Xiu, Y., Nakamura, K., Abe, M., Li, N., Wen, X-S., Jiang, Y., Zhang, D. et al., Transcriptional regulation of *Fcgr2b* gene by polymorphic promoter region and its contribution to humoral immune responses. *J. Immunol.* 2002. 169: 4340–4346.

5 Lin, Q., Xiu, Y., Jiang, Y., Tsurui, H., Nakamura, K., Kodera, S., Ohtsuhi, M. et al., Genetic dissection of the effects of stimulatory and inhibitory IgG Fc receptors on murine lupus. *J. Immunol.* 2006. 177: 1646–1654.

6 Sato-Hayashizaki, A., Ohtsuji, M., Lin, Q., Hou, R., Ohtsuji, N., Nishikawa, K., Tsurui, H. et al., Presumptive role of 129 strain-derived *Sle16* locus for rheumatoid arthritis in a new mouse model with FcgRIIB-deficient C57BL/6 genetic background. *Arthritis Rheum.* 2011. 63: 2930–2938.

7 Carlucci, F., Cortes-Hernandez, J., Fossati-Jimack, L., Bygrave, A. E., walport, M. J., Vyse, T. J., Cook, H. T. et al., Genetic dissection of spontaneous autoimmunity driven by 129-derived chromosome 1 loci when expressed on C57BL/6 mice. *J. Immunol.* 2007. 178: 2352–2360.

8 Boross, P., Arandhara, V. L., Martin-Ramirez, J., Santiago-Rober, M-L., Carlucci, F., Flierman, R., van der Kass, J. et al., The inhibiting Fc receptor for IgG, FcgRIIB, is a modifier of autoimmune susceptibility. *J. Immunol.* 2011. 187: 1304–1313.

9 Subramanian, S., Tus, K., Li, Q. Z., Wang, A., Tian, X. H., Zhou, J., Liang, C. et al., A Tlr7 translocation accelerates systemic autoimmunity in murine lupus. *Proc. Natl. Acad. Sci. USA* 2006. 103: 9970–9975.

10 Wandstrat, A. E., Nguyen, C., Limaye, N., Chan, A. Y., Subramanian, S., Tian, X.-H., Yim, Y.-S. et al., Association of extensive polymorphisms in the SLAM/CD20 gene cluster with murine lupus. *Immunity* 2004. 21: 769–780.

11 Jansson, L. and Holmdahl, R., The Y chromosome-linked "autoimmune accelerating" *Yaa* gene suppresses collagen-induced arthritis. *Eur. J. Immunol.* 1994. 24: 1213–1217.

12 Amano, H., Amano, E., Moll, T., Marinkovic, D., Ibnou-Zekri, N., Martinez-Soria, E., Semac, I. et al., The *Yaa* mutation promoting murine lupus causes defective development of marginal zone B cells. *J. Immunol.* 2003. 170: 2293–2301.

13 Panush, R. S., Edwards, N. L., Longley, S. and Webster, E., 'Rhupus' syndrome. *Arch. Intern. Med.* 1988, 148: 1633–1636.

14 Jawaheer, D., Seldin, M. F., Amos, C. I., Chen, W. V., Shigeta, R., Monteio, J., Kern, M. et al., A genomewide screen in multiplex rheumatoid arthritis families suggests genetic overlap with autoimmune diseases. *Am. J. Hum. Genet.* 2001. 68: 927–936.

15 Pisitkunm, P., Deane, J. A., Difilippantonio, M. J., Tarasenko, T., Satterthwaite, A. B. and Bolland, S., Autoreactive B cell responses to RNA-related antigens due to *TLR7* gene duplication. *Science* 2006. 312: 1669–1672.

16 Deane, J. A., Pisitkun, P., Barrett, R. S., Feigenbaum, L., Town, T., Ward, J. M., Flavell, R. A. et al., Control of Toll-like receptor 7 expression is essential to restrict autoimmunity and dendritic cell proliferation. *Immunity* 2007. 27: 801–810.

17 King, C., Tangye, S. G. and Mackay, C. R., T follicular helper (TFH) cells in normal and dysregulated immune responses. *Annu. Rev. Immunol.* 2008. 26: 741–766.

18 **Vinuesa, C. G., Sanz, I. and Cook, M. C.**, Dysregulation of germinal centers in autoimmune disease. *Nat. Rev. Immunol.* 2009. **9**: 845–857.

19 **King, C.**, A fine romance: T follicular helper cells and B cells. *Immunity* 2011. **34**: 827–829.

20 **Uysal, H., Nandakumar, K. S., Kessel, C., Carlsen, S., Burkhardt, H. and Holmdahl, R.**, Antibodies to citrullinated proteins: molecular interactions and arthritogenicity. *Immunol. Rev.* 2010. **133**: 9–33.

21 **López-Hoyos, M., Marquina, R., Tamayo, E., González-Rojas, J., Izui, S., Merino, R. and Merino, J.**, Defects in the regulation of B cell apoptosis are required for the production of citrullinated peptide autoantibodies in mice. *Arthritis Rheum.* 2003. **48**: 2353–2361.

22 **Spolski, R. and Leonard, W. J.**, Interleukin-21: basic biology and implications for cancer and autoimmunity. *Annu. Rev. Immunol.* 2008. **26**: 57–79.

23 **Bubier, J. A., Sproule, T. J., Foreman, O., Spolski, R., Shaffer, D. J., Morse, H. C. III, Leonard, W. J. et al.**, A critical role for IL-21 receptor signaling in the pathogenesis of systemic lupus erythematosus in BXSB-*Yaa* mice. *Proc. Natl. Acad. Sci. USA* 2009. **106**: 1518–1523.

24 **Rankin, A. L., Guay, H., Herber, D., Bertino, S. A., Duzanski, T. A., Carrier, Y., Keegan, S. et al.**, IL-21 receptor is required for the systemic accumulation of activated B and T lymphocytes in MRL/MpJ-Fas$^{lpr/lpr}$/J mice. *J. Immunol.* 2012. **188**: 1656–1667.

25 **Spolski, R., Kim, H.-R., Zhu, W., Levy, D. E. and Leonard, W. J.**, IL-21 mediates suppressive effects via its induction of IL-10. *J. Immunol.* 2009. **182**: 2859–2867.

26 **Fiorentino, D. F., Bond, M. W. and Moamann, T. R.**, Two types of mouse T helper cell. IV. Th2 clones secrete a factor that inhibits cytokine production by Th1 clones. *J. Exp. Med.* 1989. **170**: 2081–2095.

27 **Moore, K. W., de Waal Malefyt, R., Coffman, R. L. and O'Garra, A.**, Interleukin-10 and the interleukin-10 receptor. *Annu. Rev. Immunol.* 2001. **19**: 683–765.

28 **O'Garra, A., Barret, F. J., Castro, A. G., Vicari, A. and Hawrylowicz, C.**, Strategies for use of IL-10 or its antagonists in human disease. *Immunol. Rev.* 2008. **223**: 114–131.

29 **Hata, H., Sakaguchi, N., Yoshitomi, H., Iwakura, Y., Sekikawa, K., Azuma, Y., Kanai, C. et al.**, Distinct contribution of IL-6, TNF-a, IL-1, and IL-10 to T cell-mediated spontaneous autoimmune arthritis in mice. *J. Clin. Invest.* 2004. **114**: 582–588.

30 **Ishida, H., Muchamuel, T., Sakaguchi, S., Andrade, S., Menon, S. and Howard, M.**, Continuous administration of anti-interleukin 10 antibodies delays onset of autoimmunity in NZB/W F1 mice. *J. Exp. Med.* 1994. **179**: 305–210.

31 **Baechler, E. C., Batliwalla, F. M., Karypis, G., Gaffney, P. M., Ortmann, W. A., Espe, K. J., Shark, K. B. et al.**, Interferon-inducible gene expression signature in peripheral blood cells of patients with severe lupus. *Proc. Natl. Acad. Sci. USA* 2003. **100**: 2610–2615.

32 **Bennett, L., Palucka, A. K., Arce, E., Cantrell, V., Borvak, J., Banchereau, J. and Pascual, V.**, Interferon and granulopoiesis signatures in systemic lupus erythematosus blood. *J. Exp. Med.* 2003. **197**: 711–723.

33 **Kirou, K. A., Lee, C., George, S., Louca, K., Papagiannis, I. G., Peterson, M. G., Ly, N. et al.**, Coordinate overexpression of interferon-a-induced genes in systemic lupus erythematosus. *Arthritis Rheum.* 2004. **50**: 3958–3967.

34 **Reeve, W. H., Lee, P. Y., Weinstein, J. S., Aatoh, M. and Lu, L.**, Induction of autoimmunity by pristine and other naturally occurring hydrocarbons. *Trends in Immunol.* 2009. **30**: 455–464.

35 **Ishihara, K. and Hirano, T.**, IL-6 in autoimmune disease and chronic inflammatory proliferative disease. *Cytokine Growth Factor Rev.* 2002. **13**: 357–368.

36 **Iwakura, Y., Nakae, S., Saijo, S. and Ishigame, H.**, The role of IL-17A in inflammatory immune responses and host defence against pathogens. *Immunol. Rev.* 2008. **226**: 57–79.

37 **Banchereau, J., Pascual, V. and Palucka, A. K.**, Autoimmunity through cytokine-induced dendritic cell activation. *Immunity* 2004. **20**: 539–550.

38 **Knight, J. G., Adams, D. D. and Purves, H. D.**, The genetic contribution of the NZB mouse to the renal disease of the NZB x NZW hybrid. *Clin. Exp. Immunol.* 1977. **28**: 352–358.

39 **Zhang, D., Fujio, K., Jiang, Y., Zhao, J., Tada, N., Sudo, K., Tsurui, H. et al.**, Dissection of the role of MHC class II A and E genes in autoimmune susceptibility in murine lupus models with intragenic recombination. *Proc. Natl. Acad. Sci. USA* 2004. **101**: 13838–13843.

Abbreviations: **B6**: C57BL/6 mice · **CII**: type II collagen · **CCP**: cyclic citrullinated peptide · **FcγRIIB**: IgG Fc receptor IIB · **PNA**: peanut agglutinin · **RA**: rheumatoid arthritis · **RF**: rheumatic factor · **SLE**: systemic lupus erythematosus · **qRT-PCR**: quantitative real-time PCR · ***Yaa***: Y chromosome-linked autoimmune acceleration mutation

Full correspondence: Prof. Sachiko Hirose, Department of Pathology, Juntendo University School of Medicine, 2–1-1 Hongo, Bunkyo-ku, Tokyo 113-8421, Japan
Fax: +81-3-3813-3164
e-mail: sacchi@juntendo.ac.jp

Received: 10/10/2012
Revised: 28/11/2012
Accepted: 17/12/2012
Accepted article online: 26/12/2012

Mod Rheumatol
DOI 10.1007/s10165-012-0767-x

ORIGINAL ARTICLE

Diagnosis and treatment of primary Sjögren syndrome-associated peripheral neuropathy: a six-case series

Hiroyuki Yamashita · Toshiki Eri · Yo Ueda · Takashi Ozaki · Hiroyuki Takahashi · Takahiro Tsuno · Yuko Takahashi · Toshikazu Kano · Akio Mimori

Received: 6 July 2012 / Accepted: 30 August 2012

Abstract
Objectives The clinical and therapeutic aspects of primary Sjögren syndrome (PSS) in patients with peripheral neuropathy were analyzed and the specifics of individual case studies are discussed.
Methods We retrospectively studied six patients (four women, two men; mean age 64.5 years) presenting with PSS with peripheral neurological involvement over a five-year period (2008–2012). All patients had neurological examinations, including nerve conduction studies, somatosensory evoked potentials, and sural nerve biopsies. Treatment regimens included corticosteroids, intravenous gammaglobulin, or immunosuppressive treatment.
Results Peripheral neuropathy was observed in six (7.9 %) of 76 patients with SS as the underlying disease; three were cases of multiple mononeuropathy, two cases had sensory ataxic neuropathy, one of which was autonomic neuropathy, and one case was diagnosed as painful sensory neuropathy without sensory ataxia. Four of the six patients were diagnosed with SS after the onset of neurological symptoms. Individual peripheral neuropathies had distinct neurological, electrophysiological, and pathological characteristics. The effect of steroids and intravenous gammaglobulin differed depending on the case.
Conclusions In PSS patients, a precise diagnosis is important, because the therapeutic strategy and response varies depending on the type of neuropathy. In clinical practice, it is important to consider a diagnosis of SS when patients present with peripheral neuropathy.

Keywords Sjögren syndrome · Peripheral neuropathy · Corticosteroids · Intravenous gammaglobulin

Introduction

Sjögren syndrome (SS) is an autoimmune exocrinopathy characterized by xerophthalmia and xerostomia [1–3] and can be primary or secondary to other autoimmune diseases [3, 4]. The neurological damage observed in 20–25 % of cases is largely dominated by peripheral neuropathies [1, 5–7]. Some neurological manifestations, such as sensitive neuropathies, are specific and frequent. Here, we analyze the clinical and therapeutic characteristics of six patients with neurological signs of primary SS (PSS) and discuss some specifics of the cases.

Methods

Over a period of five years (2008–2012) we retrospectively studied six patients (four women, two men; mean age 64.5 years) presenting with PSS with peripheral neurological involvement in our Division of Rheumatic Diseases. During the same period, there were a total of 76 patients hospitalized with SS as the underlying disease. The diagnosis of PSS was established based on the criteria proposed by the Diagnostic Committee of Health and Welfare of Japan [8] or by the American-European Community [9].

All of our patients had a complete assessment to confirm the PSS diagnosis [Schirmer test, accessory salivary gland

H. Yamashita (✉) · T. Eri · Y. Ueda · T. Ozaki · H. Takahashi · T. Tsuno · Y. Takahashi · T. Kano · A. Mimori
Division of Rheumatic Diseases, National Center for Global Health and Medicine, 1-21-1 Toyama, Shinju-ku, Tokyo 162-8655, Japan
e-mail: hiroyuki_yjp2005@yahoo.co.jp

Published online: 28 September 2012

biopsy (i.e., lip biopsy), inflammatory assessment, and immunological assessment, i.e., antinuclear antibodies (ANA) and anti-SSA and anti-SSB antibodies]. Neurological examinations, nerve conduction studies (NCS), sural nerve biopsies, and somatosensory evoked potentials (SEPs) were used to confirm neurological attacks.

All patients received either steroids, immunosuppressive treatment, or intravenous gammaglobulin (IVIG) based on the subjective improvement and clinical examination data.

This study was approved by the ethics committee of our hospital.

Results

Table 1 shows the diagnostic criteria for PSS in each case. Table 2 shows the neurological findings, treatments, and outcomes for each case. Table 3 shows the results of each patient's nerve conduction studies (NCS) and somatosensory evoked potential (SEP). Detailed case reports for each patient are presented below.

Case descriptions

Patient 1

A 25-year-old woman was admitted to our hospital for thrombocytopenia, liver dysfunction, and elevated ANA titers (2,560×). Autoimmune hepatitis was excluded by liver biopsy and idiopathic thrombocytopenic purpura was excluded based on the absence of megakaryopoiesis in a bone marrow examination. SS was diagnosed based on a positive serum test result for anti-SSA antibody and the findings of a lip biopsy (Table 1). On the 9th day in the hospital, the patient complained of dysesthesia in the lateral aspect of the left thigh. On the 12th day after admission, the patient was started on oral prednisolone (PSL) at a dose of 40 mg/day based on liver dysfunction, peripheral blood cytopenia, and possible neuropathy associated with SS. PSL resulted in prompt improvement of liver function and resolution of the thrombocytopenia. However, the dysesthesia spread to both knees on the 14th day after hospitalization, and to the fingertips and lower limbs on the 15th day. Walking became difficult on the 16th day. The neurological findings included a decrease in tactile sensation and thermal nociception distributed in all of the limbs in mosaic patterns, dysesthesia, normal joint position sense in deep sensation, but decreased vibratory sensation in both upper and lower limbs, and a positive Romberg sign. The deep tendon reflexes were normal. Manual muscle testing (MMT) revealed weakness of the iliopsoas muscle. There were no abnormal reflexes (Table 2). NCS showed a decrease in all sensory nerve action potentials (SNAPs), compound muscle action potentials (CMAPs), motor nerve conduction velocity (MCV), and sensory nerve conduction velocity (SCV) in both upper and lower limbs. Initially, mononeuritis multiplex was suspected (Table 3), but nerve biopsy suggested acute or subacute axonopathy without demyelination (Fig. 1a1–2). Because of the prolonged latency of the SEP from the popliteal fossa of the lower limbs (N8o) to the S1 dorsal horn (N21), the possibility of peripheral neuropathy originating from the proximal/distal dorsal root ganglia was considered. However, the latency in spinal cord conduction and conduction from the spinal cord to the cortex were normal. Thus, mononeuritis multiplex was diagnosed. Despite steroid pulse therapy (continuous intravenous infusion of methylprednisolone at a dose of 1,000 mg/day for three days), intravenous cyclophosphamide pulse (IVCY) therapy (six pulses of cyclophosphamide at a dose of 500 mg per pulse every two weeks), and bolus IVIG therapy (two five-day courses with a daily dose of 400 mg/kg), the patient showed no significant improvement.

Table 1 The diagnostic criteria used for each case

Case	Ocular functional signs	Buccal functional signs	Ophthalmological exam		Histological criterion	Salivary scintigraphy	Immunological criterion		Number of criteria	
			Schirmer ≤5/5 mm	R.B. >4			Anti-SSA	Anti-SSB	American-European Community	The Diagnostic Committee of Health and Welfare of Japan
1	(−)	(−)	(−)	(−)	(+)	ND	(+)	(−)	2/6	2/4
2	(+)	(−)	(−)	ND	(+)	(+)	(+)	(−)	4/6	3/4
3	(+)	(−)	ND	ND	(+)	(+)	(+)	(−)	4/6	3/4
4	(+)	(−)	(−)	(−)	(+)	(+)	(−)	(−)	3/6	2/4
5	(+)	(+)	(−)	(+)	ND	(+)	(+)	(−)	5/6	3/4
6	(+)	(+)	(+)	ND	(+)	ND	(−)	(−)	4/6	4/4

R.B. Rose bengale, *Anti-SSA* anti-SS-A antibody, *Anti-SSB* anti-SS-B antibody, *ND* not done

Table 2 Clinical features of patients with Sjogren syndrome-associated peripheral neuropathy

Case	1	2	3	4	5	6
Age/sex	25/F	78/F	83/M	73/F	68/F	60/M
Diagnosis	Multiple mononeuritis			Ataxic sensory neuropathy		Painful sensory neuropathy
Interval between the onset of neurological symptoms and SS diagnosis	At the same time[a]	2 m	6 m	2 m	−3 y[b]	6 y
Neurological findings						
MMT	Decreased	Decreased	Normal	Normal	Normal	Normal
Deep tendon reflex	Normal	Sluggish or absent	Sluggish	Sluggish	Sluggish	Normal
Superficial sensation						
Touch	Decreased	Decreased	Decreased	Normal	Absent	Decreased
Temperature and pain	Decreased	Decreased	Decreased	Normal	Decreased	Decreased
Dysesthesia	+	+	+	Normal	+	+
Deep sensation						
Vibration	Decreased	Normal	Decreased	Decreased	Decreased	Normal
Joint position sense	Normal	Normal	Normal	Decreased	Decreased	Normal
Romberg test	+	Impossible	−	+	+	−
Autonomic neuropathy	−	−	−	+	−	−
Inflammation markers						
CRP (mg/dl)	0.10	12.3	0.02	4.93	0.00	0.39
ESR (mm/h)	12	108	11	ND	22	41
Treatment	Steroid pulse IVCY IVIG	PSL 1 mg/day tacrolimus 2 mg/day	IVIG	PSL 1 mg/day IVIG	IVIG	IVIG
Outcome	No change	Improved	Improved	Improved	No change	No change
Recommended therapy	Steroid and immunosuppressive agents (IVCY, etc.) IVIG should be considered if the above agents prove ineffective			Steroid IVIG		IVIG

M male, *F* female, *m* month, *y* year, *MMT* manual muscle testing, *CRP* C-reactive protein, *ESR* erythrocyte sedimentation rate, *Steroid pulse* continuous intravenous infusion of methylprednisolone at the dose of 1,000 mg/day for 3 days, *IVCY* intravenous cyclophosphamide pulse, *IVIG* intravenous gammaglobulin, *PSL* prednisolone, + positive, − negative, *ND* not done

[a] SS was diagnosed coincident with the onset of neurological symptoms

[b] SS was diagnosed three years before the onset of neurological symptoms

Patient 2

A 78-year-old woman presented with numbness and muscle weakness in all of her limbs. Two months earlier, numbness started in the left hand, which then spread to the right hand, and progressed until she was unable to walk or raise her upper limbs. She was then admitted to our division. Examination revealed dry mouth and she was diagnosed with SS based on anti-SS-A antibody positivity and lip biopsy findings (Table 1). Neurological examination revealed normal joint position sense and vibration sense, despite the presence of dysesthesia in the distal portions of all limbs and inability to walk or stand. The deep tendon reflexes were sluggish or absent. MMT showed moderate muscle weakness of both the upper and lower limbs (Table 2). NCS showed decreased amplitudes of both the compound motor action potential (CMAPs) and sensory nerve action potentials (SNAPs); however, the F waves were normal (Table 3). Furthermore, cervical-cord magnetic resonance imaging (MRI) identified T2 prolongation in the right intramedullary area at the C2–3 level, and there was evidence of concomitant myelitis (Fig. 2). The patient was diagnosed with axonal neuropathy associated with mononeuritis multiplex and myelitis caused by SS. After treatment with PSL at a dose of 30 mg/day, symptomatic improvement was obtained.

Patient 3

An 83-year-old man had begun to experience numbness in the peripheral portions of both lower limbs six months earlier. He had also experienced numbness of both hands

Table 3 Nerve conduction studies, sensory evoked potentials, and spinal cord MRI studies

Case	1	2	3	4	5	6	Normal
NCS							
Median nerve							
MCV (m/s)	40.6↓	48.0	46.4↓	50.1	52.2	56.3	>48
DL (m/s)	4.4↑	3.6	4.7	2.9	4.0	4.9	<4.0
CMAP (mV)	4.7↓	4.9↓	4.6↓	6.6	7.7	10.8	>6
SCV (m/s)	36.2↓	41.3↓	54.5	48.4	48.4	46.2	>47
SNAP (μV)	5.7↓	2.9↓	6.3↓	4.5↓	6.0↓	19.3	>12
Tibial nerve							
MCV (m/s)	36.6↓	45.1	39.3↓	41.2	41.6		>41
DL (ms)	6.0↑	3.7	4.4↓	2.4	5.5		<6.0
CMAP (mV)	2.1↓	1.6↓	11.0	14.2	22.6		>3
Sural nerve							
SCV (m/s)	35.1↓	NE↓	36.8↓	NE↓	49.0	45.2	>40
SNAP (μV)	1.8↓	NE↓	3.3↓	NE↓	2.8↓	5.0	>5
SEP							
Median nerve stimulation							
N20 latency (ms)	20.7	ND	ND	ND	20.45	ND	18.3 ± 1.5
N13 latency (ms)	17.2	ND	ND	ND	13.40	ND	13.2 ± 0.9
N9 latency (ms)	7.8	ND	ND	ND	9.85	ND	9.1 ± 0.6
Spinal cord MRI findings	Cervical, thoracic, and lumbar spinal cord MRI: no evident abnormalities	Cervical-cord MRI: T2 prolongation in the right intramedullary area at the C2–3 level and evidence of concomitant myelitis	ND	Cervical-cord MRI: no definite of intermedullary lesion, cervical spondylosis lumbar spinal cord MRI: spondyloltic spondylolisthesis of L4, accompanying disk hernia	Lumbar spinal cord MRI: no gross abnormality	ND	

NCS nerve conduction studies, *SEPs* somatosensory evoked potentials, *MCV* motor nerve conduction velocity, *SCV* sensory nerve conduction velocity, *DL* distal latency, *CMAP* compound muscle action potential, *SNAP* sensory nerve action potential, *ND* not done

in the previous month, which gradually worsened. As the patient was positive for serum anti-SSA antibody, SS-associated peripheral neuropathy was suspected and he was admitted. A definitive diagnosis of SS was made based on a positive lip biopsy, eye manifestations, and positive findings on salivary scintigraphy (Table 1). Although the MMT results were normal, superficial sensation in the peripheral portions of the upper and lower limbs and vibration sense in the lower limbs were decreased, and the deep tendon reflexes were sluggish overall. The Romberg test results were normal (Table 2). Conduction velocities and amplitudes of the median and sural nerves were decreased. Axonal neuropathy due to mononeuritis multiplex was diagnosed (Table 3). Administration of IVIG (two five-day courses at a daily dose of 400 mg/kg) yielded symptomatic relief, and slightly improved the SNAPs of the sural nerves.

Patient 4

A 73-year-old woman presented with difficulty walking and anorexia. During the previous two months, the patient had lost weight and suffered from recurrent episodes of diarrhea and constipation. Because of her general malaise during the previous month, she had become too weak to walk and was admitted. SS was diagnosed based on a positive lip biopsy and dry mouth (Table 1). The neurological findings included normal superficial sensation, decreased joint position sense in the upper and lower limbs, a positive Romberg sign, sluggish deep tendon reflexes in the lower limbs, and normal MMT results for the upper and lower limbs. Orthostatic hypotension and persistent diarrhea/constipation were detected, which are manifestations of autonomic neuropathy. Thus, the patient showed dissociated sensory disturbance, ataxic gait, and autonomic

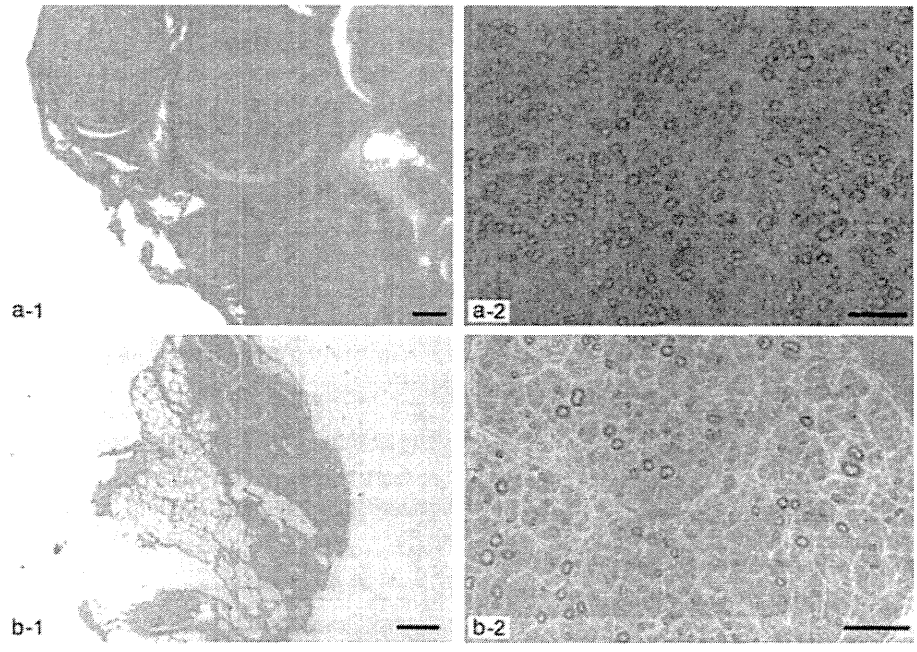

Fig. 1 Pathological findings of sural nerve biopsy in patient 1 (**a**) and patient 4 (**b**). **a-1** H&E stain (*scale bar* = 100 μl). Neither inflammatory cell infiltration nor inflammatory changes in the blood vessels was observed. **a-2** Toluidine blue stain (*scale bar* = 50 μl). There are sporadic findings suggestive of a mild decrease in the myelinated fiber density and acute axonal degeneration. Unmyelinated fibers are better preserved relative to the myelinated fibers. **b-1** H&E stain (*scale bar* = 200 μl). Neither apparent vascular necrosis nor amyloid deposition is observed. **b-2** Toluidine blue stain (*scale bar* = 50 μl). A moderate decrease in the myelinated fiber density is observed. There is no evidence of acute axonal degeneration. Unmyelinated fibers are better preserved than the myelinated fibers

neuropathy (Table 2). NCS showed decreased SNAPs in the upper limbs and loss of SNAPs in the lower limbs (Table 3). Nerve biopsy findings suggested axonopathy that appeared to be chronic with subacute changes involving myelinated fibers. These findings were consistent with the dissociated sensory disturbance, mainly of deep sensation (Fig. 1b1–2). A diagnosis of sensory ataxic neuropathy with autonomic involvement was made. IVIG therapy (one five-day course with a daily dose of 400 mg/kg) was administered, which yielded an improvement in the symptoms.

Patient 5

A 68-year-old woman was diagnosed with SS based on the presence of both dry mouth and eyes 13 years earlier. The patient had developed pollakiuria and painful urination three years earlier. She was admitted to our division for detailed examination. Interstitial cystitis was diagnosed by cystoscopy. Meanwhile, she had suffered from numbness in both lower limbs below the knees and dysesthesia in the soles for the previous ten years. The diagnosis of SS was supported by severe salivary gland dysfunction found by salivary scintigraphy (Table 1). Neurological examination revealed dysesthesia and decreased superficial sensation in the lower limbs, and the Romberg sign was positive. Although deep tendon reflexes were absent, the results of MMT were normal (Table 2). NCS showed decreased amplitudes, consistent with sensory disturbances. SEP amplitudes could not be derived from the peripheral neural components, and the latency increased with proximity to the central nervous system. Delayed stimulation conduction due to peripheral sensory disturbance was considered (Table 3). The site of disturbance was consistent with dorsal root ganglionopathy, based on the absence of motor neuropathy. Based on a tentative diagnosis of sensory ataxic neuropathy associated with SS, IVIG therapy (one five-day course at the daily dose of 400 mg/kg) was administered. However, no marked improvement was obtained, either in the clinical symptoms or in nerve conduction velocity tests.

Patient 6

A 60-year-old man had begun to experience numbness in the peripheral portions of both lower limbs six years earlier, which began to worsen two years earlier. The patient was admitted to our division with suspected connective tissue disease. A diagnosis of SS was made based on mouth and eye dryness and positive lip biopsy findings. The serum test for ANA was also positive, and chest computed tomography (CT) revealed evidence of interstitial

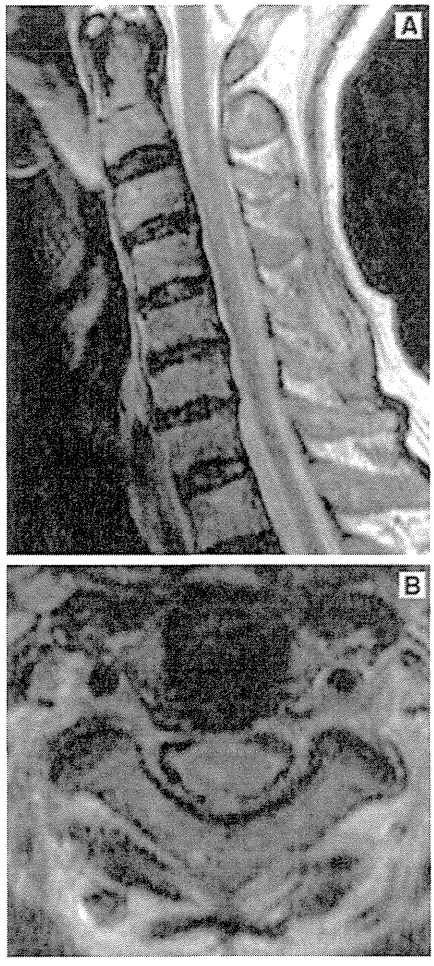

Fig. 2a–b Cervical-cord MRI findings of patient 2 (T2-weighted imaging). T2 prolongation in the sagittal section at the C2–3 level (**a**), and T2 prolongation in the right intramedullary area in the axial section (**b**) were observed. These findings are consistent with myelitis

pneumonitis. Thus, the symptoms were consistent with SS (Table 1). Neurological findings included decreased superficial sensation and dysesthesia. The deep tendon reflexes were normal, the joint position sense was normal, and the Romberg sign was negative. No evidence of autonomic neuropathy was observed, even on the tilt test (Table 2). Neither NCS nor SEP showed any abnormalities (Table 3). Thus, small-fiber neuropathy associated with SS was diagnosed. Despite the administration of IVIG therapy (one five-day course with a daily dose of 400 mg/kg), no marked improvement was obtained.

Discussion

Based on data collected from our division, peripheral neuropathy was observed in six (7.9 %) of 76 patients with SS. The calculated prevalence of peripheral neuropathy in previously published series ranges from less than 2 % to over 60 % [10, 11]. Pavlakis et al. [12] suggested that these discrepancies could be attributed to the fact that studies have been published over the last 20 years, when the diagnostic criteria for SS were still evolving. In addition, most studies were retrospective and included a relatively small number of patients. Moreover, the definition of peripheral neuropathy differed among series and was not always based on objective clinical and electrophysiological criteria. Finally, the study designs were heterogeneous.

An overlap may exist among the different peripheral neuropathies in SS, which most authors consider are related to vasculitis [7, 13–15]. Mori et al. [16] subclassified seven forms of neuropathy: sensory ataxic neuropathy, painful sensory neuropathy without sensory ataxia, multiple mononeuropathy, multiple cranial neuropathy, trigeminal neuropathy, autonomic neuropathy, and radiculoneuropathy. In the present study, we encountered three cases of multiple mononeuropathy, two cases of sensory ataxic neuropathy, one of which was autonomic neuropathy, and one case of painful sensory neuropathy without sensory ataxia.

Three patients (patients 1–3) presented with multiple mononeuropathy. According to the report of Mori et al. [16], multiple mononeuropathy occurs in 12 % of PSS-associated peripheral neuropathies. The initial symptom of mononeuritis multiplex is the acute onset of tingling or painful dysesthesia in the distal limbs. Subsequently, motor and sensory symptoms occur episodically and extend to multiple nerves. The sudden onset and pattern of mononeuritis multiplex suggests vasculitic neuropathy. When the disease underlying peripheral neuropathy is a vasculitic syndrome, increased levels of inflammatory markers are generally observed. However, two of the three patients with multiple mononeuropathy in our study were negative for inflammatory responses. This may be a feature of SS. CMAPs and SNAPs in the involved nerves were markedly reduced, suggesting axonal degeneration. Biopsy of the affected nerves often shows axonal degeneration and perivascular inflammatory infiltrates, suggesting underlying vasculitis [15]. When ataxic sensory neuropathy is considered in the differential diagnosis, as in patient 1, SEP and nerve biopsy are helpful. In cases of dorsal root ganglionitis, which causes Wallerian degeneration, the latency from the spinal cord to the cortex is prolonged. However, the latency was normal in patient 1; therefore, dorsal root ganglionitis was considered unlikely.

Two patients (patients 4 and 5) had ataxic sensory neuropathy that was characterized by impairment of deep sensory nerves without substantial motor symptoms. The initial symptoms are usually paresthesias in the digits of the foot or hand, often beginning unilaterally and then spreading to the limbs, trunk, and face. Generalized

areflexia is typically associated with sensory ataxia. Deep sensory impairment was mostly predominant with Romberg's sign in both patients. The time from the onset of symptoms to the development of full-blown sensory involvement was variable among the patients, usually ranging from months to years. With respect to nerve conduction, SNAPs in the median and sural nerves were not evoked or decreased in patient 4 or 5. In contrast, CMAPs were preserved in both patients. MCV and SCV were not slowed. These conduction studies indicated that axonal features were present in this neuropathy. Mori et al. [17] pointed out that T2*-weighted MRI sometimes demonstrates posterior column high-intensity signals that correlate in extent with the distribution and intensity of sensory involvement and sensory ataxia. Thus, as seen in patient 5, prolonged latency in the spinal cord center in the SEP test is useful in differentiating this from other types of peripheral neuropathy. Nerve biopsies characteristically show loss of myelinated nerve fibers without axonal regeneration, especially when large-diameter nerve fibers are significantly damaged. The findings of patient 4's nerve biopsy were consistent with this. Although ataxic sensory neuropathy, which is not caused by vasculitis, is not generally associated with an increase in the serum C-reactive protein (CRP) level, patient 4 had a serum CRP level of 4.93 mg/dl, suggestive of an inflammatory response. This could be attributable to the concomitant arthritic symptoms associated with the SS in this patient, and is unlikely to have been associated with the ataxic sensory neuropathy.

Patient 6 was diagnosed with painful sensory neuropathy, which is the most common type of neuropathy associated with SS [12]. The initial symptoms are typically painful dysesthesias in the most distal portions of the limbs, usually beginning unilaterally. Sensory impairment was relatively predominant with respect to superficial sensation of pain, temperature, and light touch in patient 6. Deep sensation was relatively well preserved, and motor function was also preserved. In the majority of patients, the spread of dysesthesias is chronic, occurring over months to years. In contrast to sensory ataxic neuropathy, painful sensory neuropathies in SS typically show no electrophysiologic findings [18, 19]. A decreased density of epidermal nerve fibers in skin biopsies is a common feature of small fiber neuropathy of PSS-associated painful sensory neuropathies.

In the present study, patient 4 had concomitant autonomic neuropathy, symptoms that are widely seen in SS-associated neuropathy [16]. Mori et al. [16] showed a loss of sympathetic ganglion neurons associated with T-cell invasion in an autopsied patient, which strongly supports the view that autonomic ganglion cells are primarily involved. The presence of Adie's pupils may also be attributable to ciliary ganglion cell involvement [20].

The frequency of central nervous system involvement in SS (CNS-SS) is a matter of controversy [21]. Twenty to twenty-five percent of patients with primary SS had CNS manifestations, ranging from focal central lesions to dementia and conditions that mimic multiple sclerosis [22]. Any part of the brain or spinal cord can be affected. Spinal complications are less frequent and include chronic myelopathy or acute transverse myelitis [7, 23–25]. As seen in patient 2, possible CNS involvement should be considered because of the potentially serious nature of CNS complications and the fact that some are treatable with immunosuppressive medications.

In the present study, four of the six patients were diagnosed with SS after the onset of neurological symptoms. In the remaining two patients, SS was diagnosed at the time of neurological symptom onset in one patient; in the other patient, neurological symptoms occurred three years after the diagnosis of SS. Thus, in most patients, neuropathy develops first and then the diagnosis of SS is made up to six years later, consistent with previous studies [17, 26–28]. We still do not know why the neuropathic symptoms precede the manifestations of sicca symptoms and other characteristic features in SS-associated neuropathy patients. Mori et al. [16] suggest that one possible scenario is that patients with initial neuropathic symptoms would first be referred to a neurologist rather than to a rheumatology clinic. Thus, the current diagnostic criteria for SS based on sicca syndrome may need to be re-evaluated.

Although four of the six patients in this study had anti-SS-A antibody, none of the patients tested positive for anti-SS-B antibody. According to a study in which Mori et al. [16] collected data on SS and peripheral neuropathy, there were 39 patients with anti-SS-A antibody (54.2 %) and 12 patients with anti-SS-B antibody (16.7 %) among 72 PSS patients with peripheral neuropathy. These results are consistent with the results of our study, in terms of the extremely low prevalence of anti-SS-B antibody. Mori et al. indicate that the low prevalence of anti-SS-A and anti-SS-B antibodies in their neuropathic patients may contribute to the onset of the neuropathy before the diagnosis of SS. Although the cause of the low prevalence of anti-SS-B antibody in SS patients with peripheral neuropathy remains unknown, a low sensitivity for anti-SS-B antibody in original SS may be responsible, at least in part, for the low prevalence.

The treatment of PSS neurological manifestations is not codified, and the evaluation of therapeutic efficiency is very difficult [29]. If mononeuritis multiplex is present and is a manifestation of systemic vasculitis, then aggressive therapy with steroids and immunosuppressive agents may be required [7–16]. Alexander suggests a monthly cyclophosphamide pulse for at least one year associated with initial steroid therapy [30]. Mori et al. reported that steroids